VYSOKÉ UČENÍ TECHNICKÉ V BRNĚ
BRNO UNIVERSITY OF TECHNOLOGY

FAKULTA ELEKTROTECHNIKY A KOMUNIKAČNÍCH TECHNOLOGIÍ
FACULTY OF ELECTRICAL ENGINEERING AND COMMUNICATION

ÚSTAV RADIOELEKTRONIKY
DEPARTMENT OF RADIO ELECTRONICS

NÍZKOŠUMOVÝ ZESILOVAČ PRO PÁSMO S
LOW NOISE AMPLIFIER FOR THE S BAND

DIPLOMOVÁ PRÁCE
MASTER'S THESIS

AUTOR PRÁCE — **Bc. Ivan Alejandro Benites Ayala**
AUTHOR

VEDOUCÍ PRÁCE — **prof. Ing. Miroslav Kasal, CSc.**
SUPERVISOR

BRNO 2019

VYSOKÉ UČENÍ TECHNICKÉ V BRNĚ
FAKULTA ELEKTROTECHNIKY A KOMUNIKAČNÍCH TECHNOLOGIÍ

Diplomová práce

magisterský navazující studijní obor **Elektronika a sdělovací technika**
Ústav radioelektroniky

Student: Bc. Ivan Alejandro Benites Ayala ***ID:*** 159274
Ročník: 2 ***Akademický rok:*** 2018/19

NÁZEV TÉMATU:

Nízkošumový zesilovač pro pásmo S

POKYNY PRO VYPRACOVÁNÍ:

Prostudujte teoretický návrh nízkošumového zesilovače (LNA) pro frekvenci 2.3 - 2.4 GHz. Zaměřte se na šumové přizpůsobení a vyšetřování stability zesilovače. Seznamte se s možností návrhu a simulace nízkoúrovňových zesilovačů v návrhovém a simulačním prostředí ANSYS. Zisk zesilovače nechť je větší než 20 dB, vstup a výstup nesymetrický s impedancí 50 Ohmů. Konstrukci zesilovače navrhněte ve stíněném boxu v planárním provedení na vhodném substrátu.

Zvažte otázku selektivních obvodů na vstupu zesilovače. Zesilovač realizujte, změřte a jeho parametry a porovnejte je s teoretickými předpoklady.

DOPORUČENÁ LITERATURA:

[1] HANUS, S.- SVAČINA, J.: Vysokofrekvenční a mikrovlnná technika. Brno: Skriptum FEKT VUT v Brně, 2002.

[2] ROHDE, U. L.- NEWKIRK, D. P.: RF/Microwave Circuit Design for Wireless Applications. New York: John Wiley & Sons, 2000.

[3] WHITE, J. F.: High Frequency Techniques. New York: John Wiley & Sons, 2004.

[4] RADMANESH, M. M.: Advanced RF&Microwave Circuit Design. Autor House, Bloomington, 2009.

Termín zadání: 4.2.2019 ***Termín odevzdání:*** 16.5.2019

Vedoucí práce: prof. Ing. Miroslav Kasal, CSc.
Konzultant:

prof. Ing. Tomáš Kratochvíl, Ph.D.
předseda oborové rady

ABSTRACT

This master's thesis presents the design and the realization of a low noise amplifier (LNA) for the S band of radio frequency spectrum from 2.3 GHz to 2.4 GHz. This thesis is mainly focused on stability and impedance matching networks study. Ansoft Designer and ANSYS HFSS programs are used for this design to simulate the LNA. Different low noise devices are simulated in order to find the best results for the final design. Moreover, a coaxial cavity resonator is designed in the input of the LNA and works as a band pass filter. Finally, the LNA is fabricated and its properties compared with the simulation results.

KEYWORDS

Low noise amplifier, PMA2-33LN+ monolithic amplifier, operating point, stability, matching network, noise figure, coaxial cavity resonator, interdigital band pass filter.

BENITES AYALA, Ivan Alejandro. *Low Noise Amplifier for the S Band*. Brno: Brno University of Technology, Faculty of Electrical Engineering and Communication, Department of Radio Electronics, 2019. pp. 80. Master's thesis. Supervisor: Prof. Ing. Miroslav Kasal, CSc.

DECLARATION

I declare that I have worked on this master's thesis on the topic "Low Noise Amplifier for the S Band" independently under the guidance of my thesis supervisor, using only the primary and secondary sources cited in the bibliography at the end of the work.

I further declare that, as the author of this master's thesis, I did not infringe the copyrights of third parties, in particular, I did not intervene in the personal and property copyright of others, and I am fully aware of the consequences of violation of § 11 et seq Law no. 121/2000 Coll., on copyright, rights related to copyright and amending some laws (Copyright Act), as amended, including possible criminal consequences arising from the provisions of Part II, Title VI. Part 4 of the Penal Code no. 40/2009.

Brno, 16th May 2019 .....

(Author's signature)

ACKNOWLEDGEMENT

I would like to express my sincere gratitude to my supervisor Prof. Ing. Miroslav Kasal, Csc. for his continuous support for this master's thesis, as well as for his patience, motivation, and valuable advice. I would especially like to thank my family: they have been extremely supportive of me throughout this entire process to get to this point.

Faculty of Electrical Engineering
and Communication

Brno University of Technology
Technicka 12, CZ-61600 Brno, Czech Republic

http://www.six.feec.vutbr.cz

Experimentální část této diplomové práce byla realizována na výzkumné infrastruktuře vybudované v rámci projektu CZ.1.05/2.1.00/03.0072
Centrum senzorických, informačních a komunikačních systémů (SIX)
operačního programu Výzkum a vývoj pro inovace.

TABLE OF CONTENTS

INDEX OF ILLUSTRATIONS

INDEX OF TABLES

INTRODUCTION

It is well established that low noise amplifiers (LNAs) are basic and essential functional blocks in communication system receivers of radio frequency (RF). The main function of the LNA in terms of the input of the analog processing chain is to amplify the signal without adding significant noise.

The main objective of this master's thesis is to design a low noise amplifier (LNA) for the S band from 2.3 GHz to 2.4 GHz, with a gain or amplification greater than 20 dB, a minimum insertion noise, and input and output impedance of 50 ohms.

This master's thesis is divided in two principal parts. The first part discusses essential characteristics, parameters and concepts for designing a LNA, such as noise figure, scattering parameters, stability, power gain, nonlinearities in amplifiers and impedance matching networks. In Sections 1.3 and 1.4 of this part, fundamental concepts for designing selective circuits are explained, such as microstrip band pass filters and cavity resonators.

The second part is divided in nine sections, where two designs of the LNA with different active devices have been proposed, and one of them was chosen and implemented. In this part, a microstrip interdigital band pass filter and a coaxial cavity resonator were also designed and implemented. Simulations of the LNAs and the coaxial cavity resonator have been performed using the Ansoft Designer program and HFSS (High Frequency Structure Simulator) respectively. Finally, the complete LNA design with the PMA2-33LN+ and PMA2-43LN+ monolithic amplifiers was fabricated, measured, and its properties compared with the simulation results.

1 THEORETICAL PART

1.1 About Low Noise Amplifier (LNA)

A low noise amplifier (LNA) is an electronic amplifier, which is designed to have some particular characteristics different from other amplifiers. The LNA is generally used in RF reception systems to amplify a very low-power signal and it is connected very close to the reception device (antenna) to reduce losses in the supply line.

In the design of LNA it will be essential to consider the noise, which comes from the low power signals and LNA's components. Therefore, the LNA will reduce the noise while amplifying the useful signal, thereby the amplification of the desired signal is obtained for its post-processing.

1.2 Characteristics of Low Noise Amplifiers

1.2.1 Noise Factor, Noise Figure and Noise Temperature

The noise factor (*F*) is a figure that quantifies the noise power originating internally in a two-port network. The noise factor of a network can be defined as the ratio of the available noise power from the two-port network with the internal noise sources to the available noise power without the internal noise sources [1] namely:

$$F = \frac{N_{out}}{kTBG_A}\ [-], \tag{1.1}$$

where N_{out} is the available noise power available from the two-port's output, k is the Boltzmann constant, T_0 is the temperature (standard 290 K), B is the bandwidth used in the measurement and G_A is the two-port network available gain. Noise figure (*NF*) is the noise factor expressed in dB.

$$NF = 10\,log\,F\ [dB]. \tag{1.2}$$

Yet, there is still another measure of the noise of a two-port network. Equivalent noise temperature T_e characterizes the noise properties of a two-port network in terms of Kelvins. The relation between T_e and F is:

$$F = 1 + \frac{T_e}{T_0}\ [-]\,, \tag{1.3}$$

where T_0 is the room temperature (290 K). Measure of the noise occurring in amplifiers is often performed using the Y-Factor method [2].

1.2.2 Scattering Parameters

In high frequency networks, direct measurements of voltages and currents become problematic. Therefore, the description of these networks is facilitated by incident, reflected, and transmitted voltage waves. [3]. The scattering parameters (S-parameters)

relate these waves and provide representations of the high frequency networks in RF electronics. S-parameters are also widely used for modeling of passive and active components. Furthermore, the convertibility of S-parameters allows the derivation of ABCD-, Z- and Y-parameters [4].

If an amplifier is considered as a two-port network as shown in Figure 1.1 the scattering matrix representing such a network has the following form:

$$\begin{bmatrix} V_1^- \\ V_2^- \end{bmatrix} = \begin{bmatrix} S_{11} & S_{12} \\ S_{21} & S_{22} \end{bmatrix} \begin{bmatrix} V_1^+ \\ V_2^+ \end{bmatrix}, \tag{1.4}$$

where V_1^-, V_2^- are the reflected wave voltages, V_1^+, V_2^+ are the incident wave voltages on the ports, and $S_{11}, S_{12}, S_{21}, S_{22}$ are the S-parameters that expressed using the complex numbers. The overall voltage at port 1 is $V_1 = V_1^+ + V_1^-$ and at port 2 is $V_2 = V_2^+ + V_2^-$. It should be mentioned that the DC power supply port is omitted in this kind of two-port representation. This means that S-parameters represent an amplifier for specific bias conditions. Moreover, the S-parameters provide the network description for one frequency only.

The S-parameters expressed as a set of two equations take the following form:

$$V_1^- = S_{11}V_1^+ + S_{12}V_2^+, \tag{1.5}$$

$$V_2^- = S_{21}V_1^+ + S_{22}V_2^+. \tag{1.6}$$

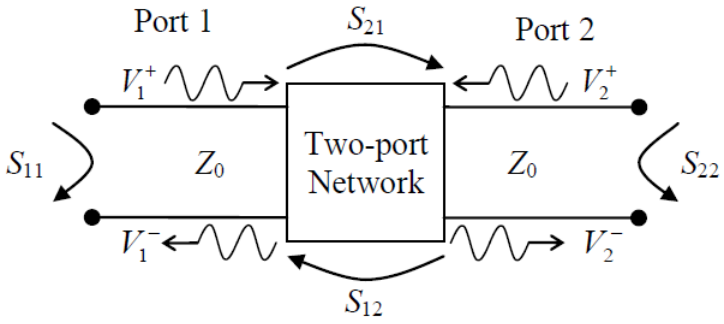

Figure 1.1 S-parameters in the two-port network.

The S_{11} parameter can be found from (1.5) as:

$$S_{11} = \left.\frac{V_1^-}{V_1^+}\right|_{V_2^+=0} \tag{1.7}$$

The condition $V_2^+ = 0$ in (1.7) means that there is not a wave coming from the port 2. In other words, we say that the port 2 is matched to a load. In majority RF systems, the termination impedance of the port two would have value 50 Ω.

The remaining S-parameters of the two port network are found a similar way:

$$S_{21} = \left.\frac{V_2^-}{V_1^+}\right|_{V_2^+=0} \tag{1.8}$$

is transmission coefficient from port 1 to port 2,

$$S_{22} = \left.\frac{V_2^-}{V_2^+}\right|_{V_1^+=0} \tag{1.9}$$

is reflection coefficient at port 2,

$$S_{12} = \left.\frac{V_1^+}{V_2^+}\right|_{V_1^+=0} \tag{1.10}$$

is the transmission coefficient from port 2 to port 1.

Considering amplifiers, the parameters S_{21} is commonly expressed in the logarithmic scale and it relates to gain. Return loss (RL), which is commonly used as the measure of input and output matching of amplifiers, can be derived for example for the input port from the parameter S_{21} as:

$$RL_{IN} = 20\log\left|\frac{1}{S_{11}}\right| \tag{1.11}$$

In other words, RL can be also understood as the decibel-difference between the incident power and reflected power.

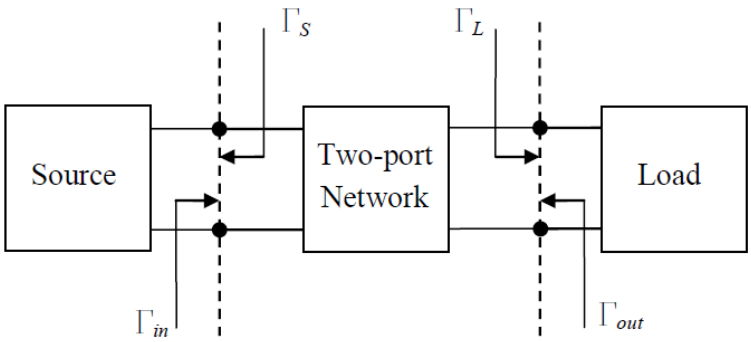

Figure 1.2 Terminated two-port network with source and load.

1.2.3 Stability

1.2.3.1 General Concept

We now consider a two-port network connected to a source and terminated with arbitrary impedances. The corresponding reference planes represented by reflection coefficients are shown in Figure 1.2. The two-port network is unconditionally stable if the magnitudes of the reflection coefficients Γ_{in}, and Γ_{out} are less than unity for passive loads [5], thus it should hold that

$$\text{for: } |\Gamma_S| < 1, |\Gamma_L| < 1, \tag{1.12}$$

$$|\Gamma_{in}| = \left|S_{11} + \frac{S_{12}S_{21}\Gamma_L}{1 - S_{22}\Gamma_L}\right| < 1, \tag{1.13}$$

$$|\Gamma_{out}| = \left|S_{22} + \frac{S_{12}S_{21}\Gamma_S}{1 - S_{11}\Gamma_S}\right| < 1, \tag{1.14}$$

From the equations 1.13 and 1.14 is apparent that Γ_S and Γ_L have an effect on the stability as the S-parameters remain constant for a particular frequency. Depending on the values of Γ_S and Γ_L the stability of the two-port network can be of two kinds, unconditionally stable or potentially unstable [4]. The unconditionally stable two-port network will never oscillate for any passive loading connected to the network. The potentially unstable two-port network may oscillate if Γ_S and Γ_L reflection coefficients do not support the stability conditions (1.13) and (1.14).

1.2.3.2 Stability Factors

Source stability factors μ_S and load stability factor μ_L determine the stability of a two-port network considering only the S-parameters.

$$\mu_S = \frac{1 - |S_{22}|^2}{|S_{22} - S_{11}\Delta| + |S_{21}S_{12}|}, \tag{1.15}$$

$$\mu_L = \frac{1 - |S_{11}|^2}{|S_{22} - S_{11}\Delta| + |S_{21}S_{12}|}, \tag{1.16}$$

$$\Delta = S_{11}S_{22} - S_{12}S_{21}. \tag{1.17}$$

Derivation of the stability factors is based on the conditions given by equations (1.13) and (1.14). It is enough to check only one of these two stability factors. Therefore the active two-port network is unconditionally stable if $\mu_S > 1$. In other words when $\mu_S > 1$ then also $\mu_L > 1$ and vice versa. In other case, when $\mu_S \leq 1$ the network is potentially unstable.

1.2.3.3 Stability Circles

The potentially unstable network will not oscillate if the Γ_S and Γ_L are selected from stable regions. The stable and unstable regions are separated by a stability circle. For example, the output stability circle represents all values of Γ_L when $|\Gamma_{IN}| = 1$. The center C_L and radius r_L of the circle (Figure 1.3) are given by:

$$r_L = \left| \frac{(S_{12}.S_{21})^*}{|S_{22}|^2 - |S_{11}.S_{22} - S_{12}.S_{21} -|^2} \right|, \tag{1.18}$$

$$C_L = \frac{(S_{22} - (S_{11}.S_{22} - S_{12}.S_{21}).{S_{11}}^*)^*}{|S_{22}|^2 - |S_{11}.S_{22} - S_{12}.S_{21} -|^2}. \tag{1.19}$$

In addition, μ_L defines the distance between the center of the Smith chart and the unstable region in the load plane (Figure 1.3).

Stable and unstable regions must be observed very carefully on the Smith chart especially if the output stability circle encloses the origin $\Gamma_L = 0$ and if the S-parameter $|S_{22}| > 1$ [4].

The potentially unstable two-port network can be made unconditionally stable by a resistive loading. Although employing the resistive loading results in overall performance degradation, it is common to apply stabilization method for potentially unstable two-port

networks [4].

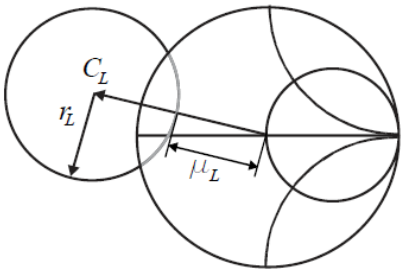

Figure 1.3 Load stability circle of a two-port plotted on the Smith chart Γ_L plane. C_L is a complex number representing the center and r_L is the radius of the circle. μ_L defines the distance between the center of the Smith chart and the unstable region.

1.2.4 Power Gain

If a two-port network is connected to a generator and to a load, four signal power levels can be identified as it is shown in Figure 1.4

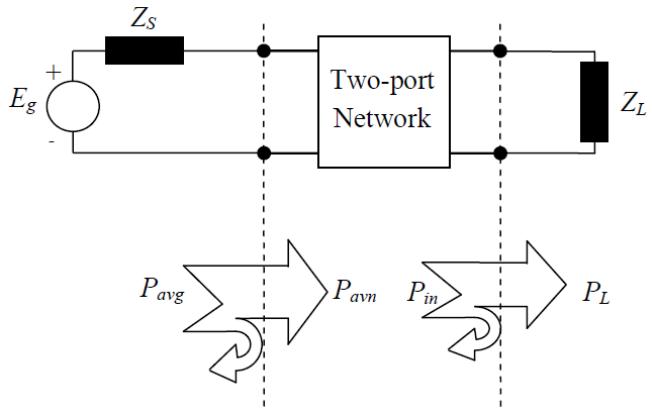

Figure 1.4 Power relations in a two-port network.

We denote these power levels at different positions of the circuit as available power from the source P_{avg}, available power from the two-port network P_{avn}, power input to the two-port network P_{in}, and power delivered to the load P_L. Knowing the power relations in every port, transducer power gain G_T, power gain G_P, and the available power gain G_A can be derived. The first mentioned gain G_T is dependent on both impedances Z_S and Z_L and has the following form:

$$G_T = \frac{P_L}{P_{avg}} = \frac{(1-|\Gamma_L|^2)|S_{21}|^2(1-|\Gamma_S|^2)}{|(1-S_{11}\Gamma_S)(1-S_{22}\Gamma_L)-S_{21}S_{12}\Gamma_L\Gamma_S|^2}, \quad (1.20)$$

The simplified version of G_T can be obtained substituting either (1.13) or (1.14) which also helps to derive G_A and G_P. For example, if we put the Γ_L equal to the complex conjugate of the output reflection coefficient of the two-port network Γ_{out} and substitute it to the equation (1.20), we obtain the available power gain G_A. As a result, the G_A has the following form:

$$G_A = \frac{P_{avn}}{P_{avg}} = \frac{|S_{21}|^2(1-|\Gamma_S|^2)}{(1-|\Gamma_{out}|^2)|1-S_{11}\Gamma_S|^2}. \quad (1.21)$$

G_P is independent of Z_S and has the following form

$$G_P = \frac{P_L}{P_{in}} = \frac{(1-|\Gamma_L|^2)|S_{21}|^2}{(1-|\Gamma_{in}|^2)|1-S_{22}\Gamma_L|^2}. \quad (1.22)$$

G_A and G_P can be used to derive the so-called gain circles which are drawn on the Smith chart. For example, in the low noise amplifier design, it is common to locate the available gain circles together with the noise figure circles.

In addition, gain relations as the Maximum Available Gain (MAG) and the Maximum Stable Gain (MSG) are often used in transistor data sheets for the description of maximum operating capabilities [5]. The first mentioned gain MAG is defined only when a transistor is unconditionally stable. The second mentioned gain MSG presents the highest theoretically achievable gain if the device is terminated by passive terminations and stabilized at the verge of instability such that stability factor μ_S or $\mu_L = 1$, then

$$MSG = \frac{S_{21}}{S_{12}}. \quad (1.23)$$

This gain, however, can not be achieved, because the required source and load terminations are situated on the circumference of the Smith chart [6].

1.2.5 Impedance Matching Networks

Impedance matching networks is a method which transforms given impedance into desired impedance in order to achieve a particular performance. The performance can be the maximum power transfer or minimum noise figure. The first mentioned performance aims to achieve maximum power transfer, thereby diminishes losses caused by impedance mismatch. The second mentioned performance aims to minimize the noise figure by matching an optimum source impedance to the impedance of a generator. The design work of matching the optimum source impedance to the generator impedance is called noise matching [7].

When designing a matching network, one should consider the following attributes [2]:

- **Complexity** – a simple topology composed of a minimum number of passive components is preferred, because it is cheaper and introduces less losses.
- **Bandwidth** – any type of matching network can be designed for a perfect match at single frequency only. Systems employing wide frequency operating range bring more complexity into the matching networks, because homogeneous conditions for every frequency component are often desired.
- **Implementation** – depending on a printed circuit board (PCB) area available and on feasibility, a matching network can be composed of stubs, lumped components, or their combinations. In addition, quarter wave transformers might be also used for impedance matching.
- **Adjustment** – adjustment components provide possibilities to optimize matching networks for different types of loading once a circuit is fabricated. For example, adjustable capacitors can be used in series or in parallel to a load.

1.2.6 Nonlinearities in Amplifiers

A small signal amplifier is considered nonlinear, if the output is a nonlinear function of the input. This happens if the input signal reaches considerably high power. As a result of that, different types of distortions occur [8]:

- Harmonic Distortion – if a sinusoidal signal is applied to a nonlinear system, the output spectrum shows frequency components which are integer multiples of the input signal.
- Cross Modulation – when two different signals from dissimilar channels with considerably different signal powers pass through a nonlinear system, then the stronger signal can interfere and damage the weaker signal. For example, this phenomenon can occur at the amplification of TV signal channels.
- Gain Compression – limits the output signal due to saturation.
- Intermodulation – occurs when the input signal composed of two or more closely spaced frequency components generate intermodulation components which interfere with the original signal, creating spectral regrowth.

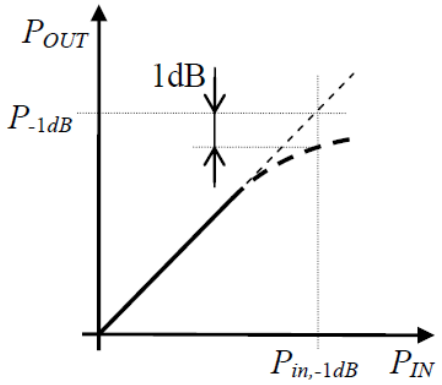

Figure 1.5 Derivation of 1-dB compression point P_{-1dB} on the log-log plot.

1.2.6.1 1-dB Compression Point

1-dB compression point is a power level which describes the power handling capabilities of an amplifier. The gain of an amplifier begins to decrease if the input signal reaches a sufficiently high level. Figure 1.7 demonstrates the situation when the gain falls off the small signal gain. The output power level under which the gain of an amplifier deviates from the small-signal gain by 1 dB is called 1-dB compression point denoted as P_{-1dB} [5].

1.2.6.2 Third Order Intercept Point

The intermodulation distortion becomes troublesome in RF systems if the working frequencies are closely separated from each other [8]. For example, if the frequencies of the input signal f_1 and f_2 are close to each other, the intermodulation products with frequencies $2f_1 - f_2$ and $2f_2 - f_1$ appear in the vicinity of f_1 and f_2. Since they are very close to each other, filtering out components $2f_1 - f_2$ and $2f_2 - f_1$ might become challenging.

The intermodulation distortion occurring in amplifiers is described in terms of a figure of merit which is called the third order intercept point (IP3). The IP3 can be

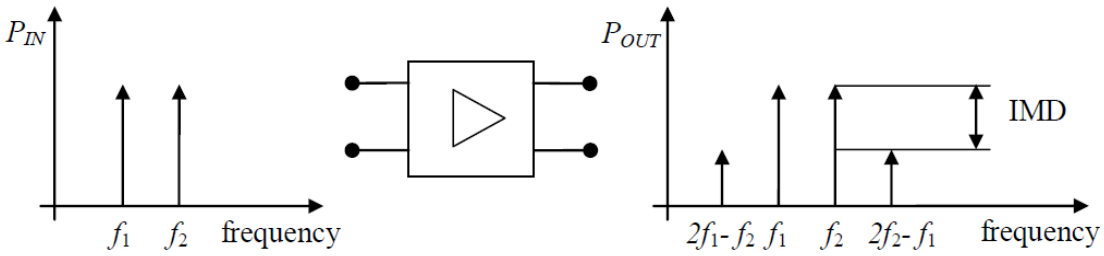

Figure 1.6 Intermodulation products by nonlinearity of amplifier.

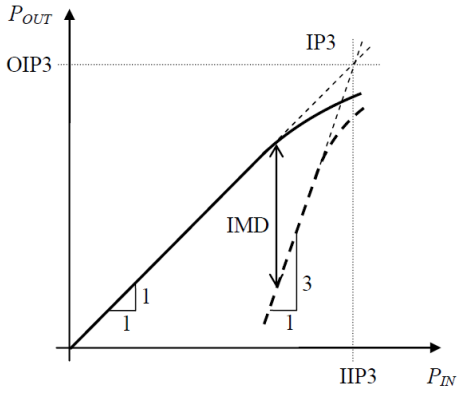

Figure 1.7 Derivation of the third order intercept point on log-log plot.

measured, for example, from the spectrum of the output signal if the input signal is composed of two different tones with a sufficiently high input power level as it is shown in Figure 1.6 [5]. The power difference between the fundamentals and the third order intermodulation products is denoted as IMD. The power of the third order intermodulation components has rapid growth with the increasing power of the input signal. This can be observed in Figure 1.7 where the curve representing the third order intermodulation products (thick dash line) is three times steeper than the curve representing the gain of the amplifier (thick solid line) [5]. The intersection of these two lines shown in Figure 1.7 represents IP3. Additionally, the horizontal coordination of IP3 is denoted as the input third-order intercept point (IIP3) and the vertical coordination is denoted as the output third-order intercept point (OIP3). OIP3 is commonly used measure of the linearity in amplifiers and mixers.

1.2.6.3 Relation of OIP3 and 1-dB Compression Point

Considering an amplifier operating at low power levels, the output signal is an amplified replica of the input signal. At high power levels, the nonlinearity of the amplifier can cause a destructive distortion of the output signal. If only the third order intermodulation products are considered as the main cause of the distortion, a quick estimate for 1-dB compression point can be derived considering only the fundamental signals and the third order intermodulation products [9].

The derivation is expressed through a difference between the fundamental signal alone and the fundamental signal including the third order intermodulation products. If

this difference is equal to 1 dB, the 1-dB compression point can be directly derived from the OIP3 as [9]:

$$P_{-1dB} \approx \text{OIP3 [dBm]} - 9.6 \text{ dB}. \quad (1.24)$$

It must be mentioned that the omission of the higher order intermodulation components (5th, 7th, and so on) might result in too optimistic estimation of P-$_{1dB}$, because the estimate is based only on the dominance of the third order components.

1.3 Microstrip Transmission Lines

Microstrip transmission line is a member of the family of planar microwave transmission lines, consists of a conducting material strip and a ground plane separated by a dielectric material [10], as shown in Figure 1.8. Microstrip line is the best known and most used type of planar transmission line in RF and Microwave circuits. This line is very popular due to its planar nature, easy manufacture, easy integration with solid state devices and great mechanical support, among others.

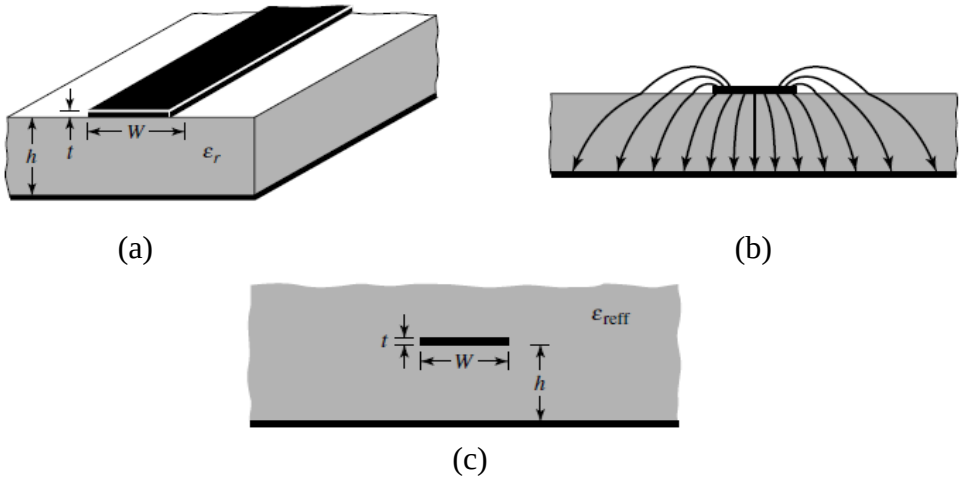

Figure 1.8 (a) Microstrip line, (b) Electric field lines, (c) Effective dielectric constant [11].

Some computational relations for analysis of microstrip structures [12]**:**

- Effective width (W_{ef}) of microstrip line (t = 0):

$$W_{ef} = \frac{2\pi h}{\ln\left(\frac{8h}{w} + \frac{w}{4h}\right)} \quad \text{for narrow microstrip } \frac{\text{w}}{\text{h}} \leq 1, \quad (1.25)$$

$$W_{ef} = w + \frac{2h}{\pi}\ln\left[17.08\left(\frac{w}{2h} + 0.85\right)\right] \quad \text{for wide microstrip } \frac{\text{w}}{\text{h}} \geq 1, \quad (1.26)$$

where w and t are the width and the height of conducting strip, respectively, and h is the height of dielectric substrate.

- Characteristic impedance (Z_0) of microstrip line:

$$Z_0 = \frac{120\pi}{\sqrt{\varepsilon_{efr}}} \frac{h}{w_{ef}}. \quad (1.27)$$

where ε_{efr} is the relative value of the effective permittivity: $\frac{\varepsilon_r+1}{2} \leq \varepsilon_{efr} \leq \varepsilon_r$.

- Determination of the dimensions *w* and *h* of the microstrip line from the known values of *Zo* and ε_r (relative permittivity):

$$\frac{h}{w} = \frac{1}{4}\left(\frac{e^H}{2} - e^{-H}\right), where\ H = \sqrt{\frac{\varepsilon_r + 1}{2}} \cdot \frac{Z_0}{60} + \frac{0.9}{\pi} \cdot \frac{\varepsilon_{r-1}}{\varepsilon_{r+1}} \quad \text{for } \frac{\text{w}}{\text{h}} \leq 1. \quad (1.28)$$

$$\frac{w}{h} = \frac{120\pi}{Z_0 \cdot \sqrt{\varepsilon_r}} - \frac{2}{\pi} - \left(\frac{2}{\pi} - \frac{\varepsilon_r - 1}{3.7\varepsilon_r}\right) \cdot \ln\left(\frac{120\pi^2}{Z_0 \cdot \sqrt{\varepsilon_r}} - 1 + 1.84\frac{\varepsilon_{r-1}}{\varepsilon_r}\right) \text{ for } \frac{\text{w}}{\text{h}} \geq 1. \quad (1.29)$$

It is important to mention that line segments shorter than a quarter of the wavelength can be replaced by an inductor or a capacitor. In the case of a line segment is terminated in a short-circuit termination, it can be replaced by an inductor with inductance L. Therefore, if the line segment is terminated in an open-circuit termination, it can be replaced by a capacitor with capacitance *C* [13].

1.4 Selective Circuits

In this section, the selective circuits refer to band pass filters. Two types of these filters are described in the following subsections such as microstrip band pass filters and cavity resonators.

1.4.1 Microstrip Band Pass Filters

1.4.1.1 Interdigital Filter

An interdigital band pass filter symbolizes an array of coupled-line resonators where each resonator element is a quarter-wavelength long at the midband frequency and is short-circuited at one end and open-circuited at the other end. This type of filter achieves good electrical characteristics such as low losses and narrow or wide passbands. The interdigital filter was chosen, designed and implemented for this LNA design because of its good characteristics and very solid and reliable construction [14].

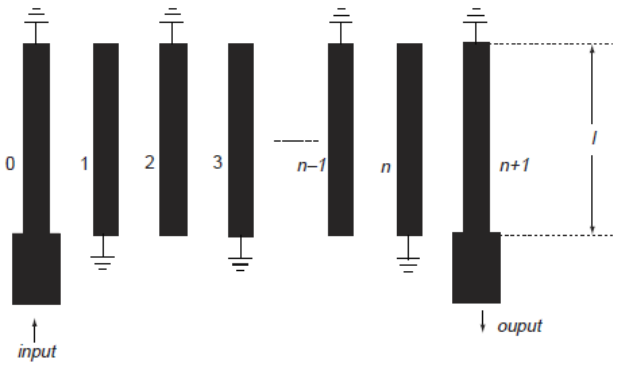

Figure 1.9 Interdigital band pass filter structure [15].

1.4.1.2 Comb-line Filter

A comb-line band pass filter consists of a set of parallel grounded resonators that are short-circuited at one end, with a lumped capacitance between the other end and ground. This type of filter with these capacitors and stab line resonators has very low losses, the bandwidth and response of this filter is governed by the coupling of each resonator to its immediate resonator. [15].

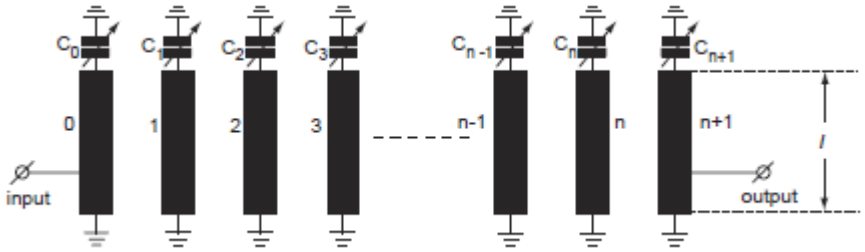

Figure 1.10 Comb-line band pass filter structure [15].

1.4.1.3 Hairpin Filter

A hairpin band pass filter consists of half-wavelength resonators folded into a U shape. This filter does not require any ground connection of resonators such as interdigital or comb-line filters. Besides, the hairpin filter is more compact that the other configurations and can be applied to miniature systems [15].

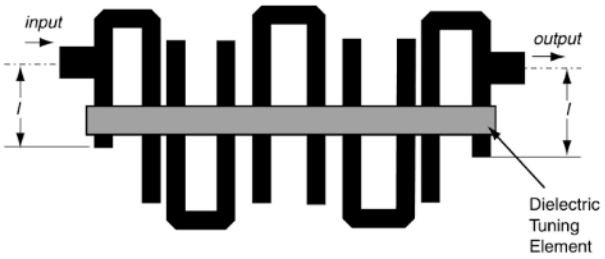

Figure 1.11 Hairpin band pass filter structure [15].

1.4.2 Cavity Resonators

Cavity resonators are the most commonly used microwave resonant circuits in the centimeter and millimeter bands. A general cavity resonator is defined as part of a space filled with a dielectric and closed with a conductive metal shell.

1.4.2.1 Rectangular Waveguide Resonator

A rectangular resonant cavity is formed by a section of rectangular waveguide of length l closed at both ends. The resonance frequency for modes TM_{mnp} and TE_{mnp} is defined as:

$$f_0 = \frac{c}{2\pi} \cdot \sqrt{\left(\frac{m\pi}{a}\right)^2 + \left(\frac{n\pi}{b}\right)^2 + \left(\frac{p\pi}{l}\right)^2}, \tag{1.30}$$

where c is the speed of light in vacuum, a, b, l are the dimensions of resonator and m, n, p are the mode numbers. In practice, rectangular cavity resonators are usually used with the simplest transverse electrical mode TE_{101}. Thus, its resonant frequency does not

depend on the height of the rectangular cavity. The change of the resonance frequency is done by changing the length of the resonator *l* [12].

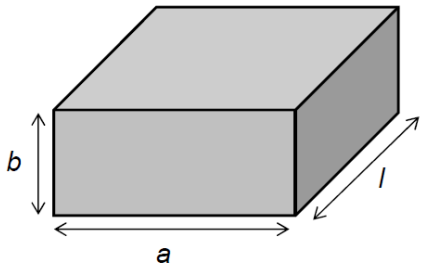

Figure 1.12 Dimensions of the rectangular waveguide resonator [16].

1.4.2.2 Circular Waveguide Resonator

A circular waveguide cavity is most useful in various microwave applications. Most commonly, it is used in wave meters to measure frequency, it has a high Q factor and affords greater resolution. It consists of a section of a circular waveguide of radius *a* and length *l*, with end plates to provide short circuit.

The resonance frequency of the circular waveguide cavity for *TE* and *TM* modes is given by [12]:

$$f_0{}^{TM} = \frac{c}{2\pi} \cdot \sqrt{\left(\frac{\alpha_{mn}}{a}\right)^2 + \left(\frac{p\pi}{l}\right)^2}, \tag{1.31}$$

$$f_0{}^{TE} = \frac{c}{2\pi} \cdot \sqrt{\left(\frac{\alpha'_{mn}}{a}\right)^2 + \left(\frac{p\pi}{l}\right)^2}, \tag{1.32}$$

where *c* is the speed of light in vacuum, *a* is the radius of circular waveguide cavity, *l* is the length of resonator, *m*, *n*, *p* are the mode numbers, α_{mn} is the solution of Bessel's function of the first kind and α'_{mn} is its derivation.

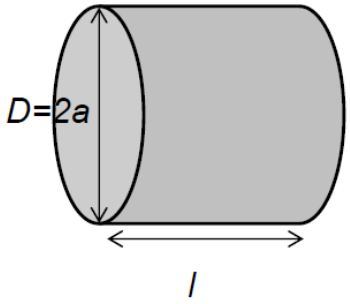

Figure 1.13 Dimensions of the circular waveguide resonator [16].

1.4.2.3 Coaxial Resonator

A coaxial resonator is formed by coaxial cavity, that is to say, a section of coaxial line closed by short-circuit or open-circuit terminals at the two ends becomes a coaxial cavity.

The coaxial cavity shorted at both ends is a half-wavelength (λ/2) coaxial cavity and the coaxial cavity with a short-circuit terminal at one end and an open-circuit terminal at the other end is a quarter-wavelength (λ/4) coaxial cavity [17].

Coaxial resonators operate exclusively with the dominant *TEM* mode. The resonance frequency of this coaxial resonator is determined by the relation [12]:

$$f_0^{TEM} = \frac{cp}{2l}, \tag{1.33}$$

where c is the speed of light in vacuum, l is the length of resonator and p is the mode number (for basic mode $p = 1$).

Relation for characteristic impedance of a coaxial cable is defined by:

$$Z_0 = \frac{U}{I} = \frac{60}{\sqrt{\varepsilon_r}} \cdot \ln\frac{R_0}{r_0}, \tag{1.34}$$

where $\frac{U}{I}$ is the amplitude relation of voltage and current (complex form), ε_r is the dielectric permittivity, R_0 is the inner dimension of resonator coating and r_0 is the outer dimension of central conductor.

If the relation $\frac{R_0}{r_0}$ can achieve a ratio equal to 3.6, a minimal attenuation results per unit length. Therefore, if this ratio is replaced in equation (1.34), the characteristic impedance of the coaxial cable for the minimal attenuation is equal to:

$$Z_0 . \sqrt{\varepsilon_r} = 77\ \Omega. \tag{1.35}$$

As was mentioned previously, the coaxial resonator is used as half-wavelength or quarter-wavelength. Construction of both resonators are shown in Figure 1.14. The quality factor (Q_0) of the half-wavelength coaxial resonator (λ/2) is defined by [12]:

$$Q_0 = \frac{2R_0}{\delta} \cdot \frac{\ln\frac{R_0}{r_0}}{1 + \frac{R_0}{r_0} + \frac{4R_0}{l} \cdot \ln\frac{R_0}{r_0}}, \tag{1.36}$$

where δ is the depth of penetration into conductive walls of the cavity at the resonance frequency, l is the length of resonator, R_0 is the inner dimension of resonator coating and r_0 is the outer dimension of central conductor.

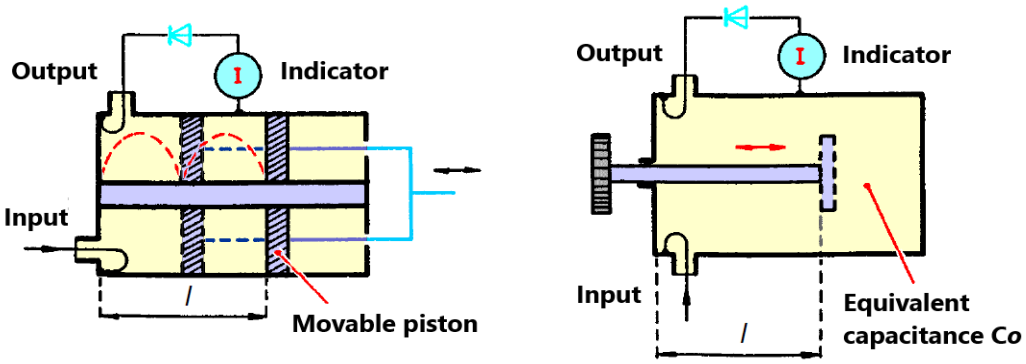

(a) (b)

Figure 1.14 (a) Half-wavelength resonator, (b) Quarter-wavelength resonator [16].

The quarter-wavelength coaxial resonator (λ/4) uses resonance properties of the short-circuited quarter-wavelength line. As it can be observed in the drawing structure in Figure 1.14 (b), the central conductor is inserted into the waveguide and the resonance occurs within the insertion length [12].

$$l \approx (2p + 1)\frac{\lambda_0}{4}, \tag{1.37}$$

where p is the mode number and λ_0 is the resonance wavelength.

A capacitance C_0 is produced between the end of the middle conductor and the opposite base of the resonator, which reduces the resonance length l. Sometime this capacitance is intentionally increased (for example, by extending the central conductor or adding a capacitive disk) to reduce overall dimensions of the resonator [12].

2 PRACTICAL PART

2.1 Choice of Substrate

The PCB material which will be used is Arlon CuClad 217 substrate. The principal advantage of this material is its good performance in high frequency band of radio frequency spectrum (RF), where this LNA design will work for S band. Additionally, the Faculty of Electrical Engineering and Communication of Brno University of Technology provides this kind of material.

Properties:

- Substrate: Arlon CuClad 217.
- Thickness: 30 mil (0.762 mm).
- Relative Permittivity (Dielectric constant): E_r = 2.17.
- Low Dissipation Factor (Electrical loss): tan δ = 0.0009.

2.2 Choice of Amplifier

The criteria for choosing the proper amplifier have been: the minimum noise (NF), the best gain (G), the highest output third order intercept (IP3) and the highest output power at 1 dB gain compression ($P\text{-}_{1dB}$); all of these characteristics are analyzed at frequency range of this LNA design for the S band. This master's thesis evaluates different low noise amplifiers of different producers according to the Table 2.1.

Two LNA designs were proposed: The PMA2-33LN+ and PMA2-43LN+ monolithic amplifiers produced by Mini-Circuit company were chosen as main active devices for the first LNA designing. For the second LNA designing, the ATF-54143 amplifier produced by Avago company was selected as main active device. The following sections of the practical part explain and show in detail the LNA designs with the respective active devices.

Table 2.1 List of different low noise amplifiers with their parameters and characteristics according to the producers.

Transistor	*f* [GHz]	*T* [°C]	NF [dB]	*G* [dB]	*T* [°C]	*f* [GHz]	IP3 [dBm]	1 dB [dBm]	S_{11}	S_{22}	Material	Producer
PMA2-43LN+	1.1-4	-65 → 150	**0.63**	**17.99**	25	2.4	**32.98**	**19.6**	14.74	10.58	SnAgNi E-PHEMT	Mini-circuits
PMA2-33LN+	0.4-3	-65 → 150	**0.47**	**11.62**	25	2.3	**38.54**	**19.11**	15.27	21.76	SnAgNi E-PHEMT	Mini-circuits
ATF-54143	0.1-18	-65 → 150	**0.5**	**16.6**	25	2	**36.2**	**20.4**	17	20.37	E-PHEMT GaAs	Avago
ATF-55143	0.1-18	-65 → 150	0.6	17.7	25	2	24.2	14.4	17.01	20.05	E-PHEMT GaAs	Avago
MGF4921AM	1.0-16	-55 → 125	0.35	15.2	25	2.4	21				InGaAs HEMT	Mitsubishi electric
NE3509M04	1.0-6	-65 → 150	0.4	17.5	25	2		14			GaAs FET	CEL (California Eastern Laboratories)
ATF-551M4	0.45-20	-65 → 150	0.46	17	25	2	24.1	14.6	3.05	7.31	E-PHEMT GaAs	Avago
ATF-35143	0.45-10	-65 → 160	0.29	12	25	2.5	21	10	2.05	7.13	PHEMT	Avago
ATF-38143	0.45-10	-65 → 160	0.28	13	25	2.5	22	12	3.35	11.37	PHEMT	Avago
ATF-58143	0.45-6	-65 → 150	0.51	15	25	2.4	30.5	19	4.01	14.42	PHEMT	Avago
BFP720-DS	>0.15	-55 → 108	0.5	21.5	25	2.4	22	6			SiGe:C bipolar tr.	Infineon
SKY65050-372LF	0.45-6	-65 → 125	0.65	15.5	25	2.4	23.5	10.5	18.5	14	PHEMT	SKYWORKS
SKY67151-396LF	0.7-3.8	-40 → 150	0.5	19	25	2.5	36	19.7	11	20	GaAs HEMT	SKYWORKS
SAV-541+	0.45-6	-65 → 150	0.39	17	25	2.4	33.1	19.2			E-PHEMT GaAs	Mini-circuits

2.3 Design of Microstrip Interdigital Band Pass Filter

A microstrip interdigital band pass filter was chosen in order to work between the two stages of this LNA design. This type of filter was chosen due to its good performance in high frequencies, such as moderate loss, rather high attenuation in limits of bands and simple construction. This design of the band pass filter consists of two coupled microstrip lines of approximately a quarter wavelength. These lines were shortened with a trimmer capacitor as it is shown in Figure 2.1.

2.3.1 Length Calculation of Microstrip Lines

Requirements:

- Center frequency of band pass filter equal to 2.35 GHz.
- Input and output impedance of 50 Ω.

Consideration:

- Trimmer capacitor 1 pF – 3 pF; value for the calculation is equal to 2 pF.

Approximate length determination of microstrip line sections:

- Thomson's relationship:

$$L = \frac{1}{4 \cdot \pi^2 \cdot f^2 \cdot c}\ [H], \tag{2.1}$$

where *f* is the center frequency of the LNA equal to 2.35 GHz, *c* is the capacitance equal to 2 pF. Therefore, *L* is:

$$L = \frac{1}{4 \cdot \pi^2 \cdot (2.35 \cdot 10^9)^2 \cdot (2 \cdot 10^{-12})} = 2.293\ nH.$$

- Calculation of specific inductance *Lo* of microstrip line:

Wave delay on the line:

$$TpD = \frac{1}{v} = \frac{\sqrt{Er}, eff}{c}\ [-], \tag{2.2}$$

where ε_r, *eff is* the effective dielectric constant (in this case 1.85), *c* is the speed of light in vacuum equal to $3 \cdot 10^8$ m/s and *v* is the wave velocity in the substrate.

$$TpD = \frac{\sqrt{1.85}}{3 \cdot 10^8} = 4.534 \cdot 10^{-9}[-].$$

Specific inductance Lo:

$$Lo = Zo \cdot TpD\ \left[\frac{H}{m}\right], \tag{2.3}$$

where Zo is the characteristic impedance equal to 50 Ω.

$$Lo = 50\,\Omega \cdot 4.534 \cdot 10^{-9} = 226.7 \cdot 10^{-9}\frac{H}{m}.$$

Thus, the length of the microstrip lines is:

$$\mathrm{l} = \frac{L}{Lo}[m], \tag{2.4}$$

where L is the Thomson's relationship and Lo is the specific inductance:

$$\mathrm{l} = \frac{2.293 \cdot 10^{-9}}{226.7 \cdot 10^{-9}} = 10.11mm.$$

2.3.2 Simulation of Band Pass Filter

The interdigital band pass filter was simulated in the Ansoft Designer program at the center frequency *fo* = 2.35 GHz. The dimensions obtained from the microstrip line segments such as the length and the width can be observed in Figure 2.1.

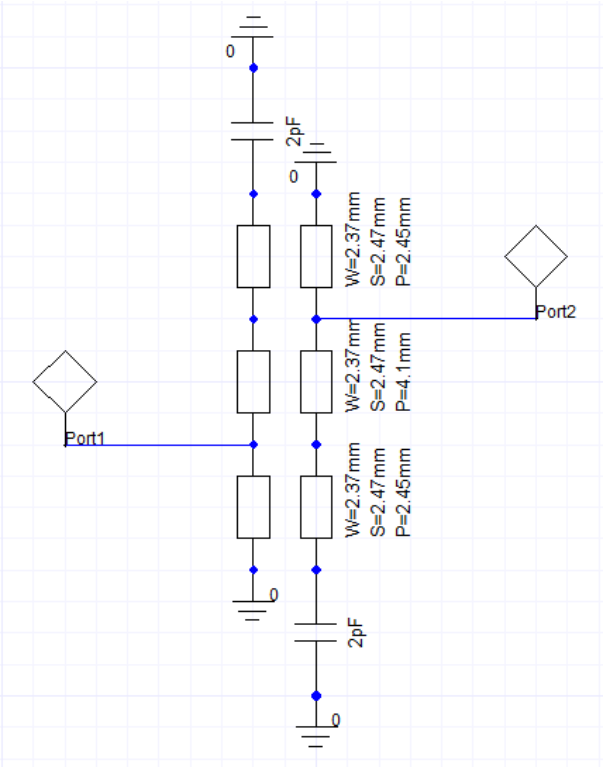

Figure 2.1 Interdigital band pass filter in Ansoft Designer program.

In Figure 2.2 the Scattering parameters can be observed; the S_{21} parameter shows an attenuation equal to -0.28 dB, and the S_{11} parameter (reflection coefficient at port 1) equal to -31 dB. The band pass filter has a bandwidth equal to 160 MHz (-3 dB cutoff frequency).

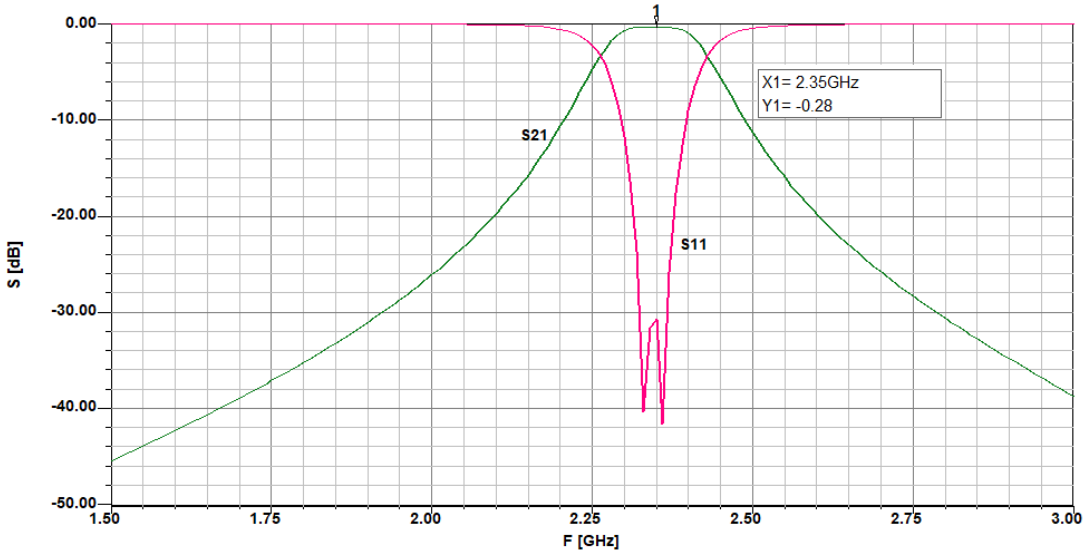

Figure 2.2 Scattering parameters (S_{21} and S_{11}).

2.4 Design of Coaxial Cavity Resonator

In order to obtain a proper selectivity for this LNA design, a quarter-wavelength coaxial resonator (λ/4) was chosen for the input due to its good performance in high frequencies such as the S band of RF spectrum. For this LNA design, it was decided to use a coaxial cavity resonator with a square outer structure and a circular inner structure as can be observed in Figure 2.3.

2.4.1 Characteristic Impedance Calculation of Coaxial Cavity with a Square Outer Structure and Circular Inner Structure

In this part, some calculations and considerations for this design of the coaxial cavity resonator with a square outer structure are mentioned. The characteristic impedance of this type of coaxial cavity resonator is defined by [21]:

$$Zo = 138 \cdot \log\left(1.079 \cdot \frac{D}{d}\right)[\Omega], \tag{2.5}$$

where D is the length of the side of the outer structure, d is the diameter of the inside circular structure.

Approximate relation for the minimum attenuation:

$$\frac{D}{d} \approx 3.6\,[-], \tag{2.6}$$

taking into account this relation for the minimal attenuation, the dimensions of the coaxial cavity resonator were chosen and determined such that the length D is equal to 24 mm and the diameter d is equal to 7 mm. Therefore, the characteristic impedance of this cavity resonator for minimal attenuation is:

$$Zo = 138 \cdot \log\left(1.079 \cdot \frac{24}{7}\right) = 78{,}4\ \Omega.$$

2.4.2 Cylindrical Capacitor Calculation

The internal cylindrical resonator of this structure is made of brass material because of its good properties in soldering; the input and the output terminals were soldered in this part of the resonator. Furthermore, an adjustable screw will be displaced from the top of the structure to the internal cylindrical resonator in order to tune the center frequency equal to 2.35 GHz. Therefore, a capacitance *C* is generated when this adjustable screw is displaced in the internal resonator and can be calculated by [22]:

$$C = \frac{2\pi \cdot k \cdot \varepsilon_0 \cdot L}{\ln\left(\frac{b}{a}\right)}[F], \tag{2.7}$$

where ε_0 is the vacuum permittivity equal to $8.854 \cdot 10^{-12}\, F/m$, *a* is the inner conductor diameter equal to $2.5 \cdot 10^{-3} m$, *b* is the outer conductor diameter equal to $5 \cdot 10^{-3} m$, *L* is the length of displacement of the screw in the internal resonator equal to $2.1 \cdot 10^{-3} m$ (value obtained in the simulation) and *k* is the dielectric constant or relative permittivity of dielectric material between inner and outer conductor, in this case equal to 2.1 for Teflon (PTFE). Therefore, the capacitance generated is:

$$C = \frac{2\pi \cdot 2.1 \cdot 8.854 \cdot 10^{-12} \cdot 2.1 \cdot 10^{-3}}{\ln\left(\frac{5 \cdot 10^{-3}}{2.5 \cdot 10^{-3}}\right)} = 0.35\, pF.$$

2.4.3 Simulation of Coaxial Cavity Resonator

ANSYS HFSS 13.0 (High Frequency Structure Simulator) was used to enhance the coaxial cavity resonator design. The values shown below are the final results obtained in the simulation and used in the implementation of this coaxial cavity resonator. Figure 2.3 shows the external and the internal structure of this coaxial cavity resonator.

Figure 2.3 (b) shows the top view, where the side of external structure is equal to 24 mm and the diameter of the central resonator is equal to 7 mm. Figure 2.3 (a) shows the front view, where, the height of the external structure is equal to 25 mm (approx. 78% of $\lambda/4 = 32$ mm) and the height of the central resonator is equal to 21.2 mm. Furthermore, as previously mentioned, this coaxial cavity resonator has an adjustable screw on the top of the structure in order to tune the center frequency equal to 2.35 GHz.

For the input and the output coupling, the tapped resonator option was used. This type of coupling was chosen because it works over a broad range of bandwidths and its construction is more feasible. The height coupling of the input and output is equal to 8 mm and 10 mm respectively (values obtained in the simulation): Both are measured from the bottom side of the structure as can be observed in Figure 2.3 (a).

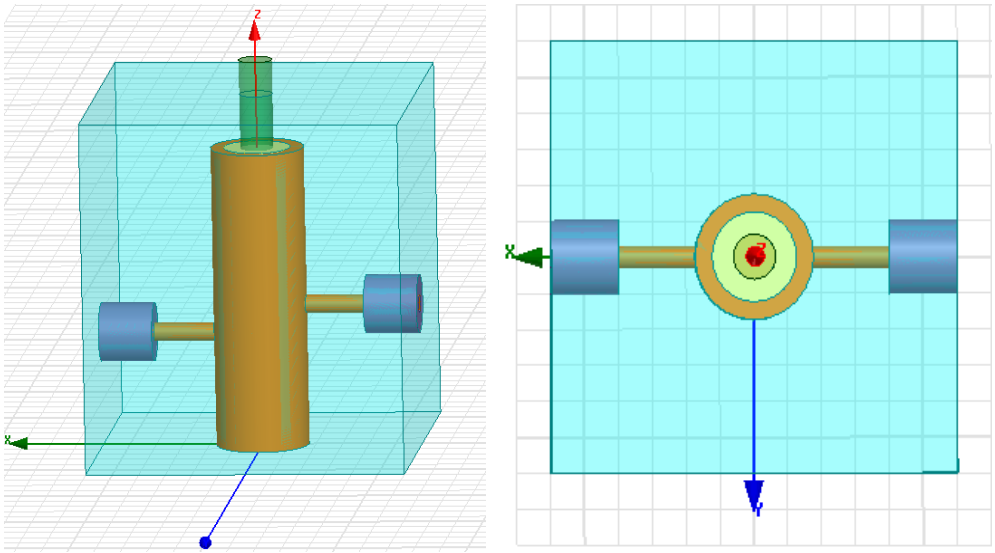

(a) (b)

Figure 2.3 Coaxial cavity resonator in HFSS – (a) Front view, (b) Top view.

Figure 2.4 shows the Scattering parameters at the center frequency of 2.35 GHz, the S_{21} parameter has an attenuation equal to -0.06 dB, and the S_{11} parameter (reflection coefficient) is equal to -39.2 dB. The coaxial cavity resonator has a bandwidth equal to 210 MHz approximately (-3 dB cutoff frequency).

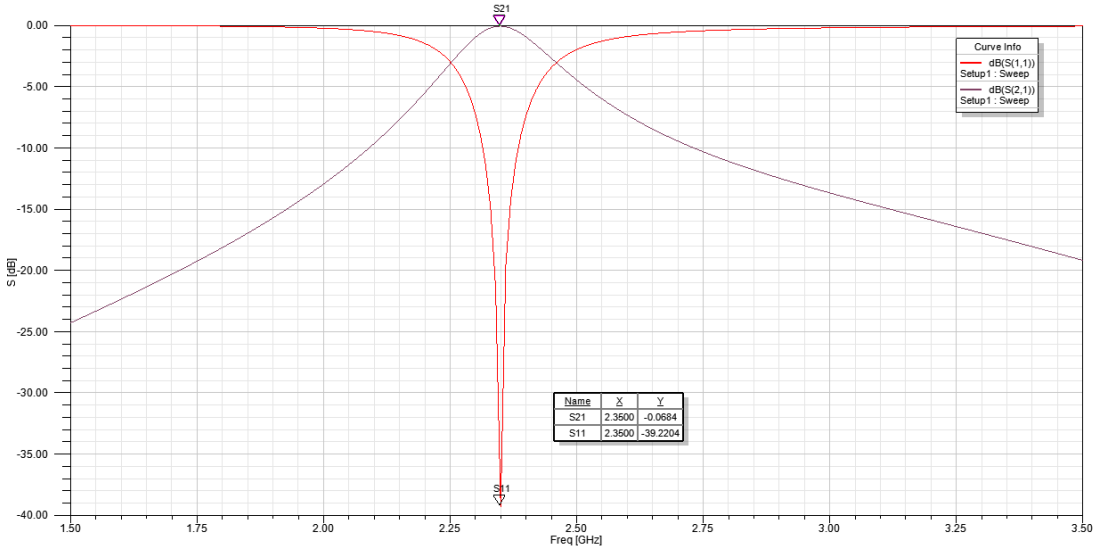

Figure 2.4 Simulation of coaxial cavity resonator – S-parameters (S_{21} and S_{11}).

Figure 2.5 shows the tuning at the center frequency of 2.35 GHz when the adjustable screw is displaced in the internal structure of the coaxial cavity resonator with a length or depth of displacement equal to 2.1 mm.

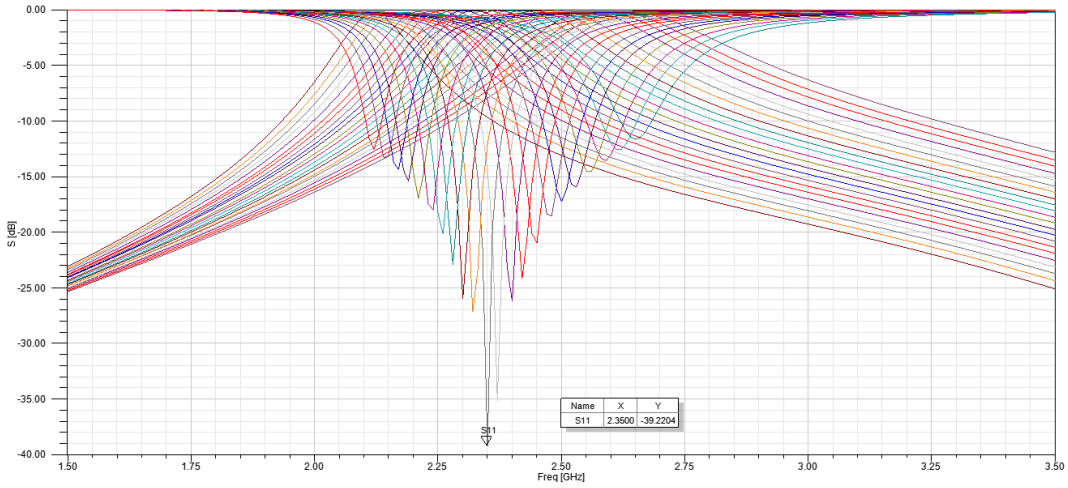

Figure 2.5 Center frequency tuning at 2.35 GHz.

2.5 Design 1 and Simulation of LNA

As it was previously mentioned, the PMA2-33LN+ and the PMA2-43LN+ monolithic amplifiers produced by Mini-Circuit company were chosen as main active devices for this first LNA designing. The PMA2-33LN+ amplifier has been used in first stage because it has a minimum noise in the frequency range from 2.3 GHz to 2.4 GHz, which is required in the input of the LNA. The PMA2-43LN+ amplifier has been used in second stage because of its high gain and power in the same frequency range, which is also required in the output of this LNA design.

2.5.1 Stage 1 of LNA (PMA2-33LN+)

2.5.1.1 Operating Point and Bias Circuit

The operating point and the bias circuit were chosen based on the manufacture's recommendation [18]. The operating point values are V_d = 3 V and I_d = 56 mA; and the bias circuit scheme with its respective values is shown in Figure 2.6 and Table 2.2.

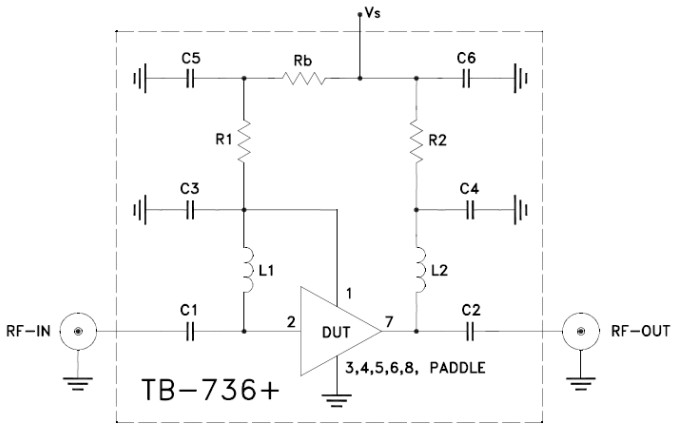

Figure 2.6 Manufacture's recommended application and characterization test circuit (Mini-Circuits producer) [18].

Table 2.2 Component values for manufacture's recommended application [18].

Component	Value	Size
C1, C2	100 pF	0402
C3, C6	4.7 uF	0402
C4	33 pF	0402
C5	Not Used	-
L1, L2	33 nH	0402
R1	0 Ω	0402
R2	10 Ω	0603
Rb	4.02 kΩ	0402

2.5.1.2 Amplifier Stability

This section focuses on the study of the PMA2-33LN+ monolithic amplifier stability. To verify and show the amplifier stability, the Ansoft Designer program is used. This program simulates the properties of this amplifier as a two-port network. Therefore, different graphs and schemes are observed such as the Scattering parameters, the Rollett's stability factor (K) and the stability circles on the Smith chart for the respective analysis of this amplifier.

Figure 2.7 shows the basic schema of the PMA2-33LN+ amplifier stability in Ansoft Designer, which is analyzed independently without other components. Next Figure 2.8 shows the Rollett's stability factor (K), it indicates the stability of the amplifier for values greater than 1. In this case, it is observed that amplifier is stable throughout the working frequency range of the amplifier, from 0.1 GHz to 3 GHz.

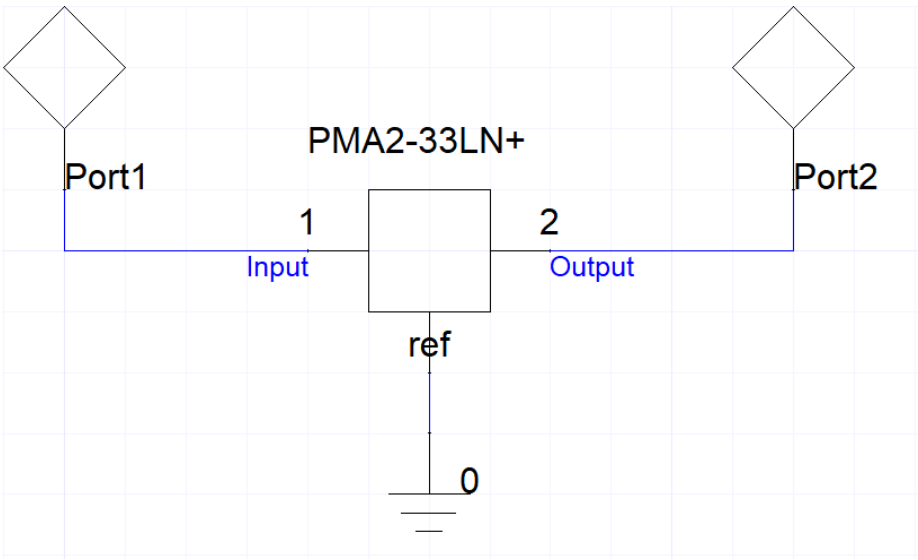

Figure 2.7 Monolithic amplifier PMA2-33LN+ (Ansoft Designer).

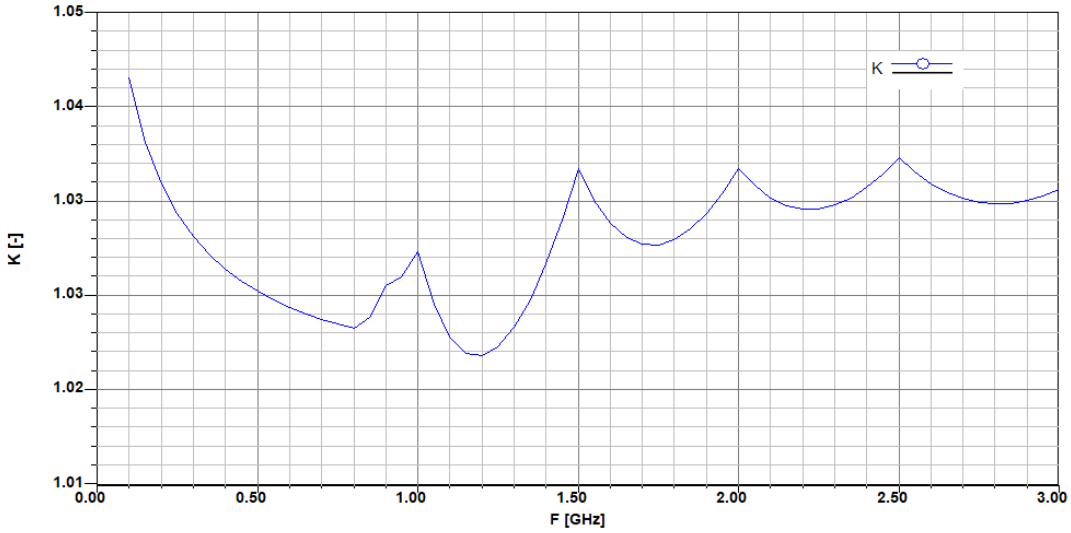

Figure 2.8 Rollett's stability factor (K) – Stable amplifier.

Other way to verify the amplifier stability is using the K-factor Circle for Source (KCS) and K-factor Circle for Load (KCL) on the Smith chart. These factors indicate that there is stability when both circles KCS and KCL are out of the Smith chart. Figure 2.9 shows the stability of the amplifier as both circles KCS and KCL are out of the Smith chart.

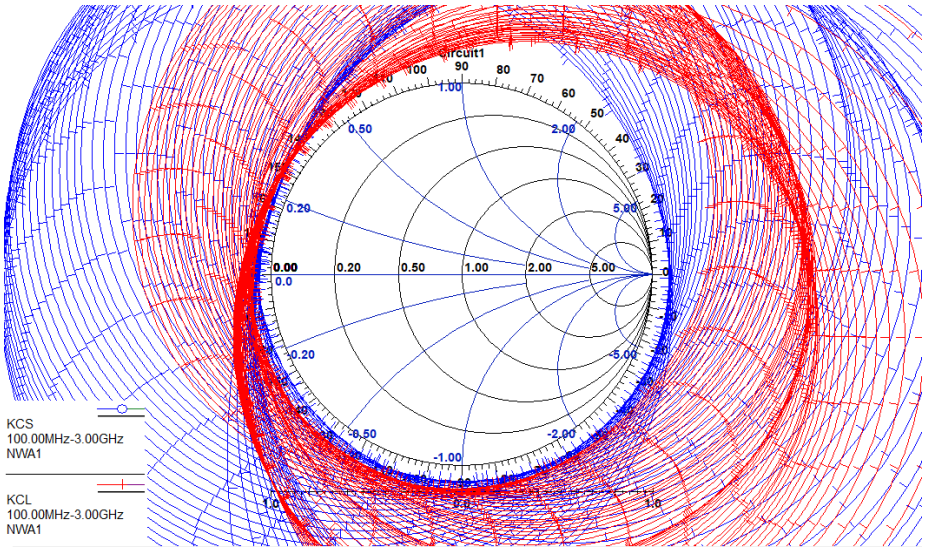

Figure 2.9 KCS and KCL stability circles on the Smith chart – Stable amplifier.

Figure 2.10 shows the complete stability of the PMA2-33LN+ amplifier with connection of biasing networks recommended by Mini-Circuit company in Ansoft Designer program. The capacitors equal to 100 pF are modified in the next step in order to find the proper impedance matching networks.

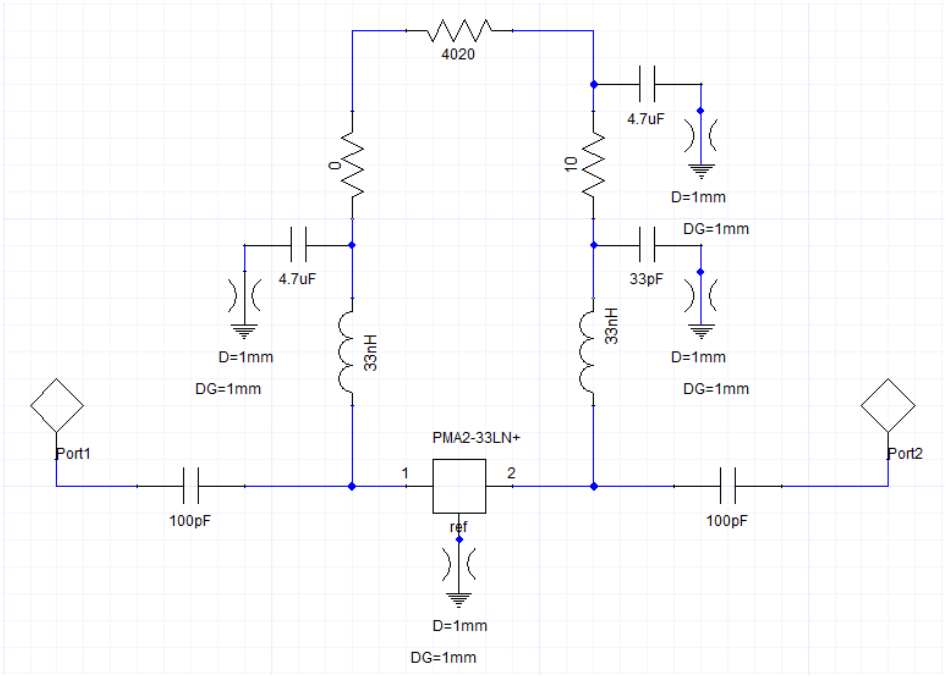

Figure 2.10 PMA2-33LN+ amplifier with bias circuit.

Figure 2.11 shows the complete stability of the transistor by Rollet's stability factor (K) at the shown frequency range where the center frequency of 2.35 GHz is included.

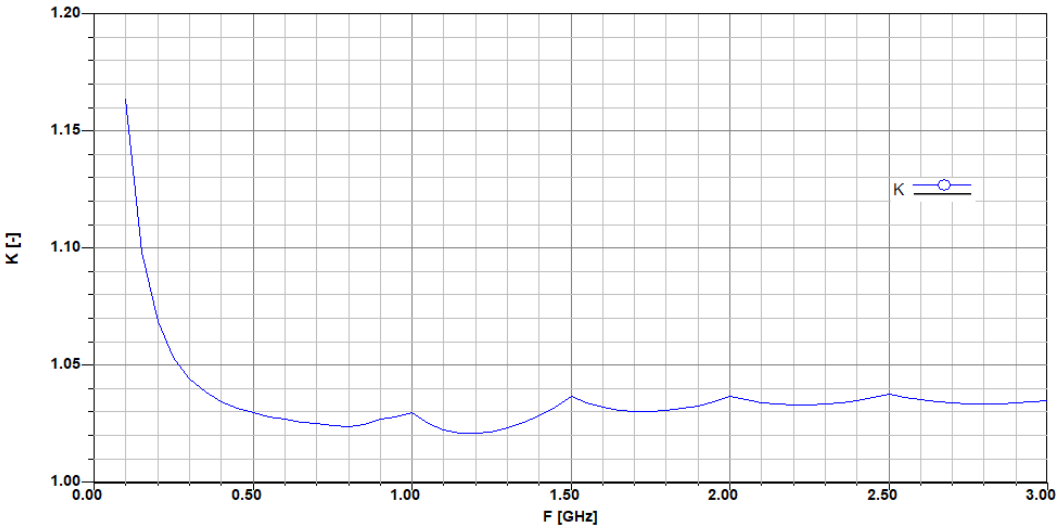

Figure 2.11 Rollett's stability factor (K) – Stable amplifier.

It is also possible to observe the transistor stability by the stability circles on the Smith chart as shown in Figure 2.12, in this case at frequency range from 2.3 GHz to 2.4 GHz. The KCS and KCL stability circles are outside of the Smith chart, which are the conditions for the transistor stability.

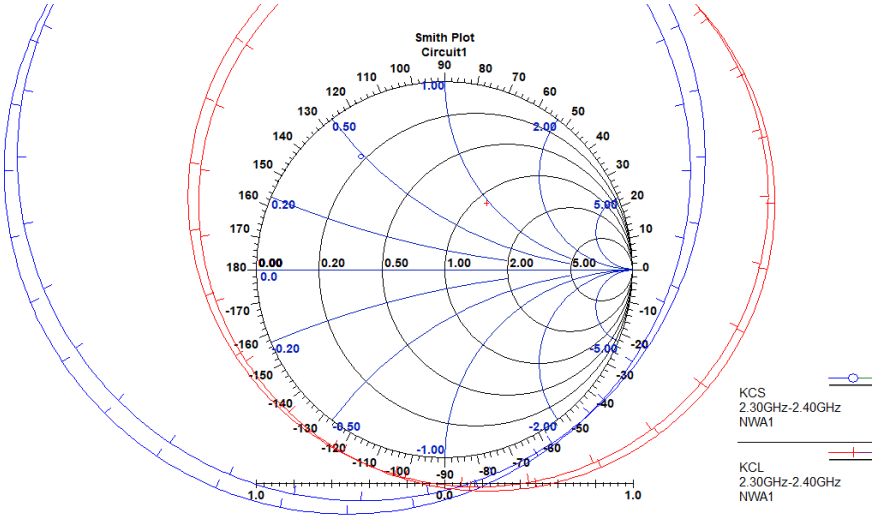

Figure 2.12 KCS and KCL stability circles on the Smith chart from 2.3 GHz to 2.4 GHz – Stable amplifier.

2.5.1.3 Impedance Matching Networks

As it was mentioned in Section 1.2.4, the impedance matching is a method that transforms given impedance into desired impedance in order to achieve a particular performance. A tool known as “Smith Tool” provided by Ansoft Designer was used to obtain matching networks for the input and output of the PMA2-33LN+ amplifier. The Smith Toll needs to be configured in advance.

To achieve the input impedance matching with impedance of 50 Ω, it was necessary to set the LNA center frequency of operation at 2.35GHz. Afterwards, the noise parameter was selected with reference value of minimum noise figure (F_{min}) equal to 0.33 dB.

The next step was selecting the Available Gain Circle for Source (GACS) with reference value less than 12.28 dB, which is the maximum gain for this condition. In this way, the circles of noise and GACS were obtained on the Smith chart. The value of GACS was set in order to obtain an intersection between the circle of GACS and the center of the circle of the noise, the value set was 11.17 dB.

Subsequently, it was possible to choose the suitable components for the input impedance matching, taking into account the center point of the Smith chart and the intersection between the circle of GACS and the center point of the circle of noise as the beginning and final of the selection of components respectively. The result of the steps mentioned can be observed on the Smith chart in Figure 2.13.

The obtained input impedance matching was a capacitor equal to 2.40 pF connected in series to a microstrip line with length P = 10.48 mm and width W = 2.34 mm. The connection of the input impedance matching network is shown in Figure 2.15.

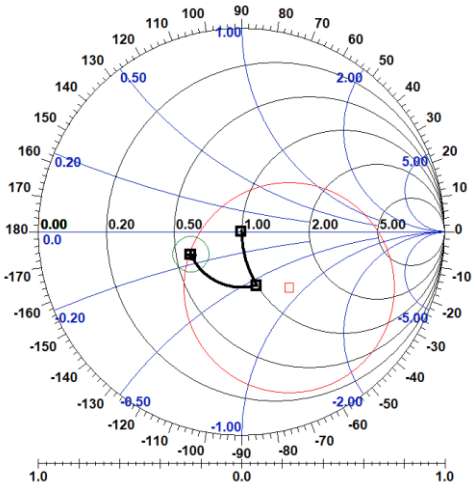

Figure 2.13 Smith tool – Input impedance matching.

To achieve the output impedance matching with impedance of 50 Ω, the same steps were executed as for the input impedance matching and a new configuration was added for obtaining the Available Gain Circle for Load (GACL), which had the same reference value as the GACS (equal to 11.17 dB).

After obtaining the GACL, the intersection between the GACS circle and the center point of the circle of noise was selected in order to obtain a reference point into the GACL circle. Finally, after these steps, it was possible to obtain the conjugation (marker point) of the previous point obtained from the GACL circle.

This new point was the initial reference for the suitable components chosen and the middle of the Smith chart was the final reference. The result of the steps mentioned above can be observed on the Smith chart in Figure 2.14.

The output impedance matching obtained was a capacitor equal to 0.954 pF connected in series to an inductor equal to 2.89 nH. This capacitor is at the same time connected in parallel to output of the PMA2-33LN+ amplifier. The connection of the output impedance matching network is shown in Figure 2.15.

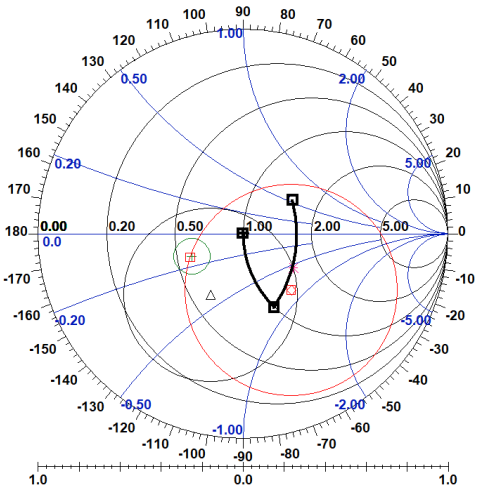

Figure 2.14 Smith tool – Output impedance matching.

Figure 2.15 shows the scheme of the first stage of LNA with impedance matching networks obtained for the input and output. The dimensions of microstrip line were obtained by tool "Microstrip single" by the Ansoft Designer, in which it was necessary to set the value of characteristic impedance, the electrical length in degrees, the center frequency and the parameters of substrate. As previously mentioned, the substrate used for this LNA designing is Arlon CuClad 217. The dimensions of microstrip line obtained are shown in the scheme below.

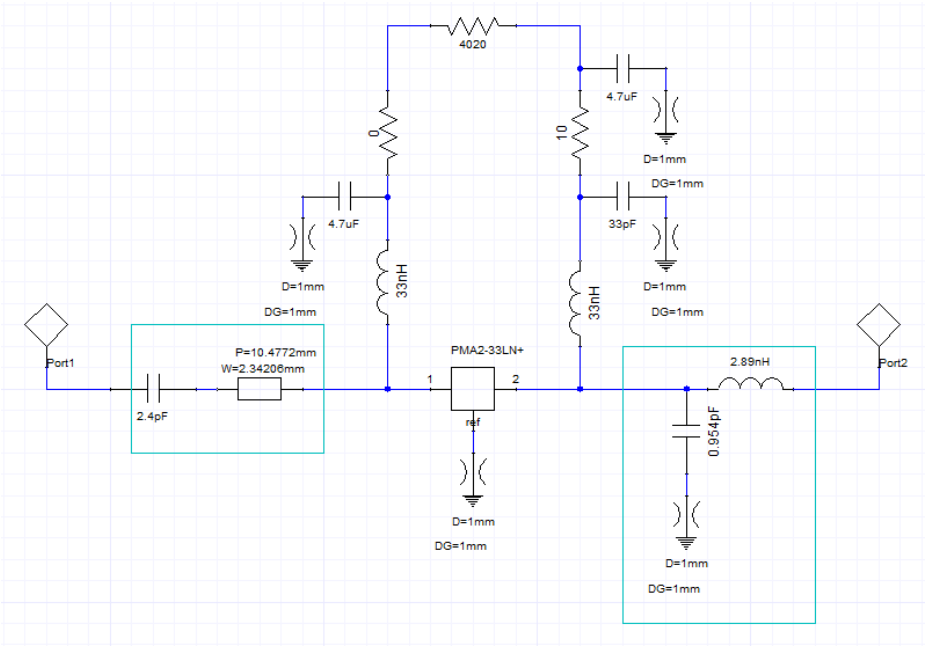

Figure 2.15 Scheme of the first stage of the LNA with impedance matching networks for input and output.

Figure 2.16 shows the value of the noise figure (NF) and the value of the minimum noise figure (F_{min}) for the LNA at the center frequency of 2.35 GHz after setting of the impedance matching networks. The graph shows that value of the noise figure is equal to the value of the minimum noise figure: $\mathrm{NF} = \mathrm{F_{min}} = 0.34$ dB, which indicates that the impedance matching networks were properly designed.

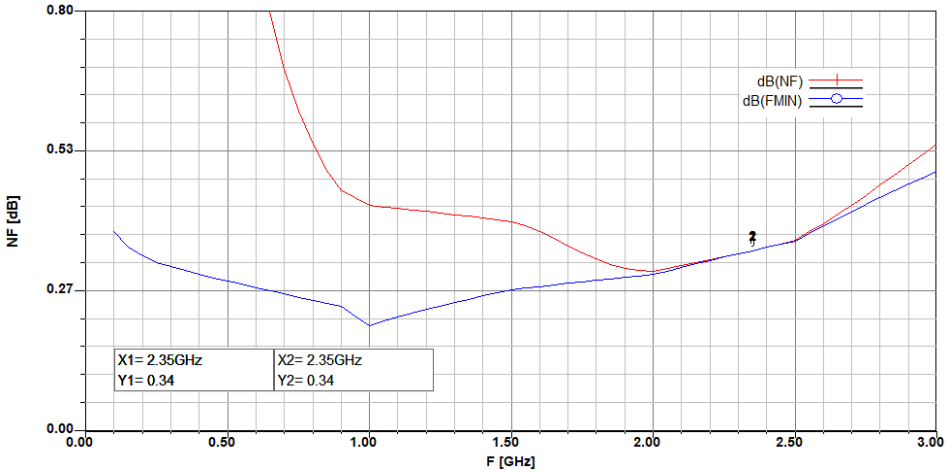

Figure 2.16 Noise figure (NF) and minimum noise figure (F_{min}) with matching networks.

The next Figure 2.17 shows the Scattering parameters of the LNA at the center frequency of 2.35 GHz, where the gain obtained is equal to 11.18 dB (S_{21} parameter).

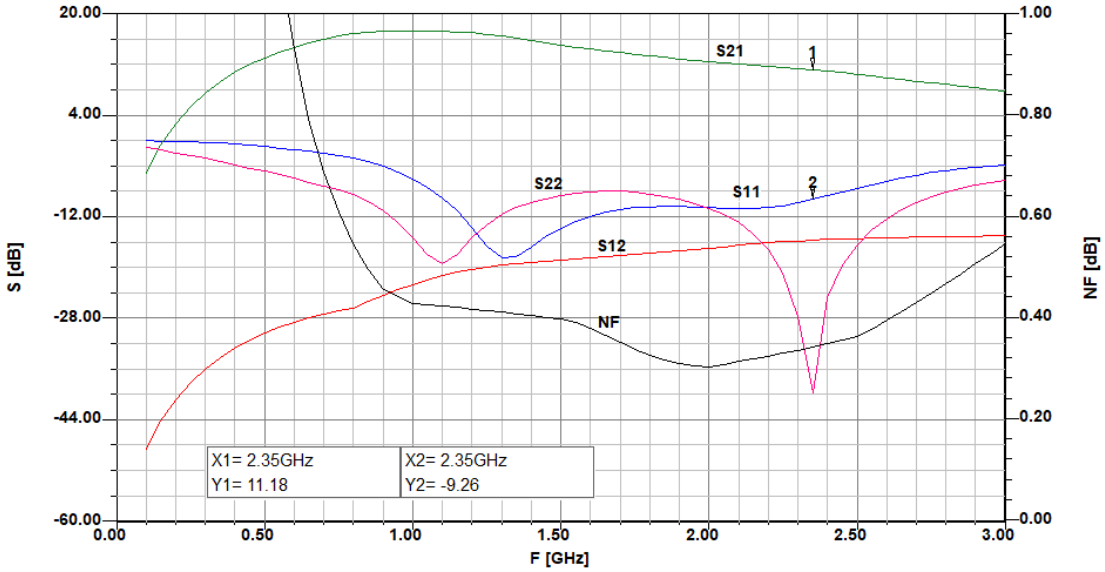

Figure 2.17 S-parameters of the first stage at the frequency range from 0.1 GHz to 3 GHz.

2.5.2 Stage 2 of LNA (PMA2-43LN+)

2.5.2.1 Operating Point and Bias Circuit

The operating point and the bias circuit were also chosen based on the manufacture's recommendation [19]. The operating point values are V_d = 5 V and I_d = 50 mA; and the bias circuit scheme with its respective values is shown in Figure 2.18 and Table 2.3.

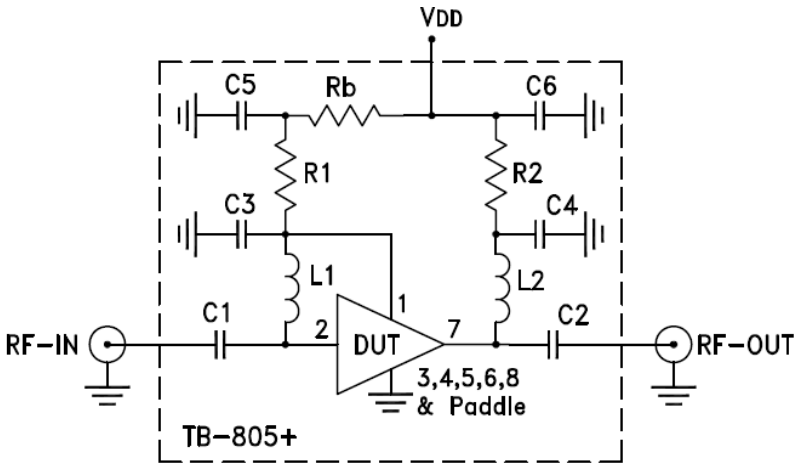

Figure 2.18 Manufacture's recommended application and characterization test circuit (Mini-Circuits producer) [19].

Table 2.3 Component values for manufacture's recommended application [19].

Component	Value	Size
C1, C2	1000 pF	0402
C5, C6	4.7 uF	0402
C3, C4	100 pF	0402
L1	10 nH	0402
L2	8.2 nH	0402
R1	49.9 Ω	0402
R2	0 Ω	0603
Rb	5.11 kΩ	0402

2.5.2.2 Amplifier Stability

Figure 2.19 shows the complete stability of the PMA2-43LN+ amplifier with connection of biasing networks recommended by Mini-Circuit company in Ansoft Designer program. The capacitors equal to 1000 pF are modified in the next step in order to find the proper impedance matching networks.

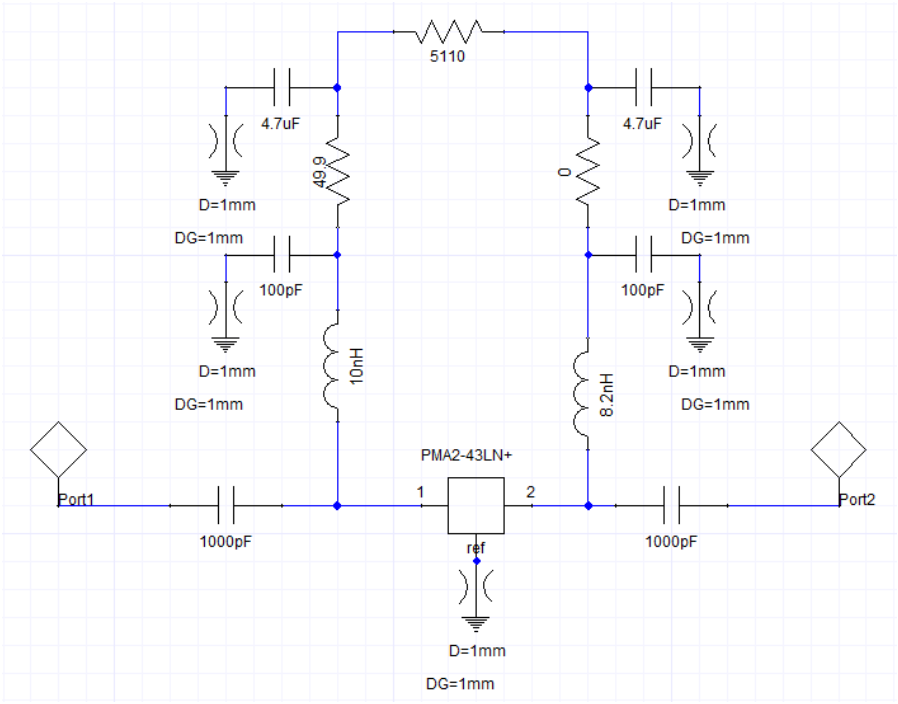

Figure 2.19 PMA2-43LN+ amplifier with bias circuit.

The Figures 2.20 and 2.21 show the ways of verifying the amplifier stability in Ansoft Designer, which were previously explained, such as the Rollett's stability factor (K) and the stability circles on the Smith chart (KCS and KCL), respectively. It can be observed that in both graphs the PMA2-43LN+ amplifier is stable.

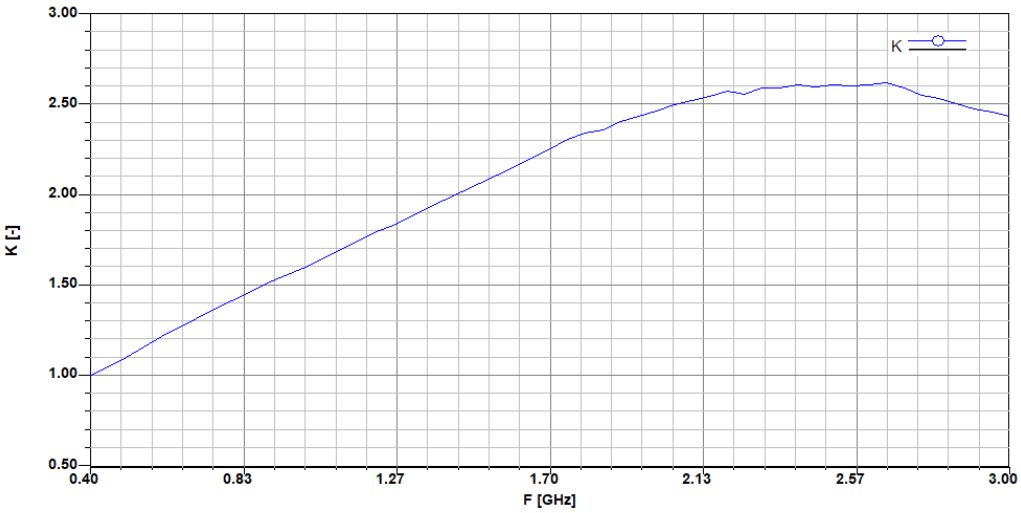

Figure 2.20 Rollett's stability factor (K) – Stable amplifier.

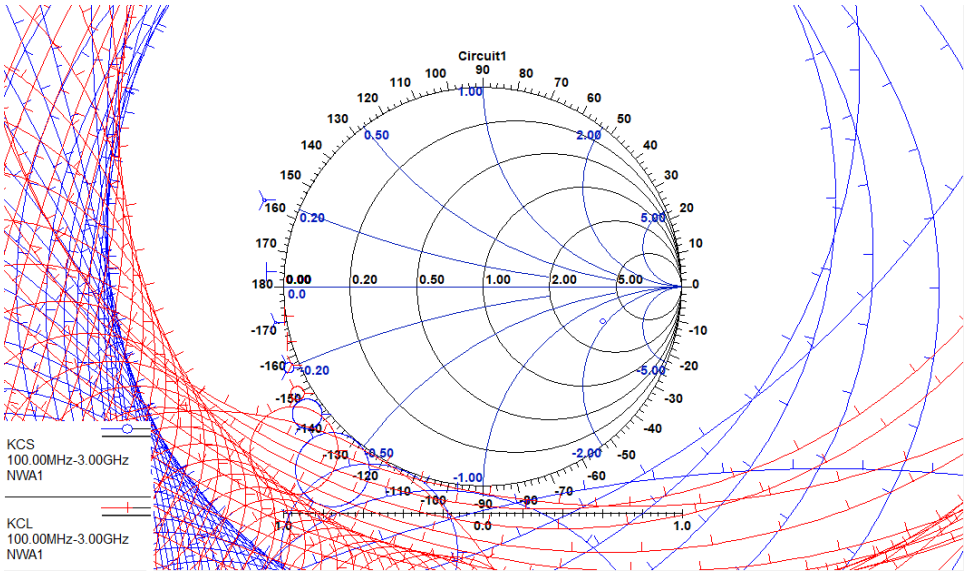

Figure 2.21 KCS and KCL stability circles on the Smith chart – Stable amplifier.

2.5.2.3 Impedance Matching Networks

To achieve the input impedance matching it was necessary to set the LNA center frequency of operation at 2.35 GHz. After that, the Available Gain Circle for Source (GACS) was selected with reference value equal to 19.14 dB, which is the maximum gain for this condition.

Afterwards, it was possible to choose the suitable components for the input impedance matching, taking into account the center point of the Smith chart and the circle of GACS (in the lower half of Smith chart) as the beginning and final of the selection of components respectively, such as shown on the Smith chart in Figure 2.22. The input impedance matching obtained was a capacitor equal to 1.28 pF connected in series to a microstrip line with length P = 0.36 mm and width W = 2.34 mm. At the same time, this capacitor is connected in parallel to the input of this second stage of LNA as can be observed in Figure 2.23.

To achieve the output impedance matching the same steps were executed as for the input impedance matching but a new configuration was added for obtaining the Available Gain Circle for Load (GACL), which had the same reference value as the GACS and maximum gain equal to 19.14 dB.

After obtaining the GACL, it was also possible to obtain its conjugation. This new point was the initial reference for the suitable components chosen for the output impedance matching and the middle of the Smith chart was the final reference (in the upper half of Smith chart). The result of the steps mentioned can be observed in Figure 2.22. Three components were obtained for the output impedance matching. They are connected in series, a capacitor equal to 2.68 pF, a microstrip line with length P = 9.20 mm and width W = 2.34 mm, and other capacitor equal to 1.7 pF. At the same time, this last capacitor is connected in parallel to the output of the PMA2-43LN+ amplifier.

The complete connection of the input and output impedance matching networks is shown in Figure 2.23.

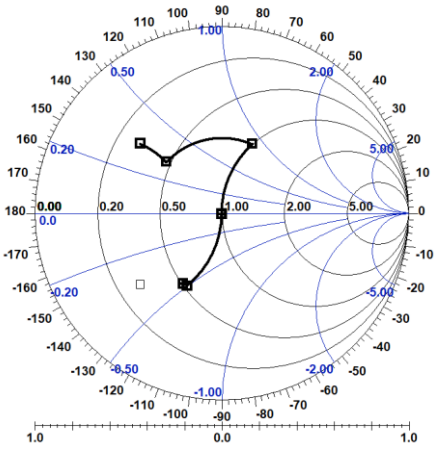

Figure 2.22 Smith Tool – Input and output impedance matching.

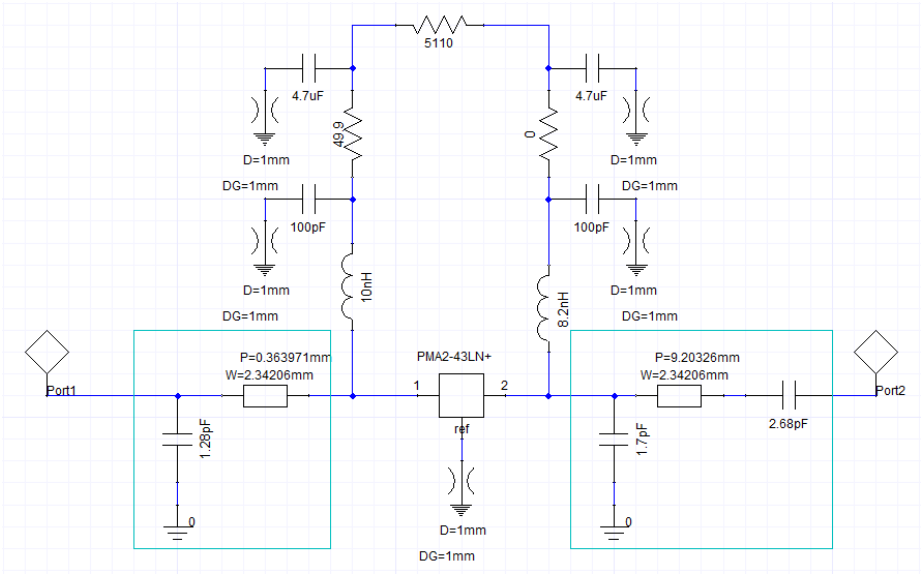

Figure 2.23 Scheme of the second stage of the LNA with impedance matching networks for the input and the output.

Figure 2.24 shows the Scattering parameters of the LNA at the center frequency of 2.35 GHz, where the gain obtained is equal to 19.13 dB (S_{21} parameter).

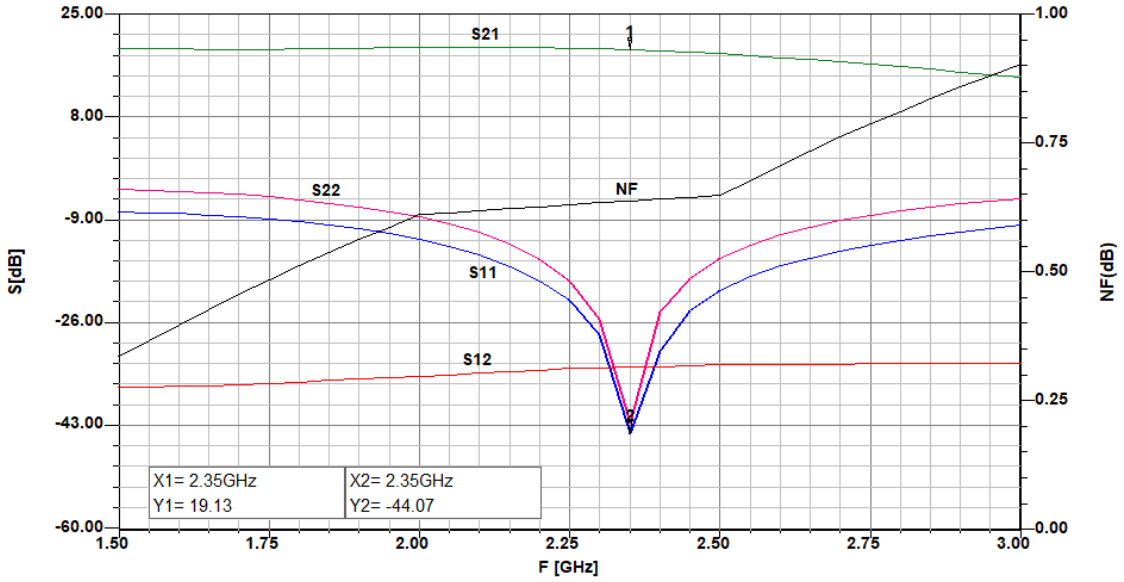

Figure 2.24 S-parameters of the second stage at the frequency range from 1.5 GHz to 3 GHz.

2.5.3 LNA Results with Band Pass Filter

Figure 2.25 displays the scheme of the LNA design with two stages and microstrip interdigital band pass filter in the middle of these stages.

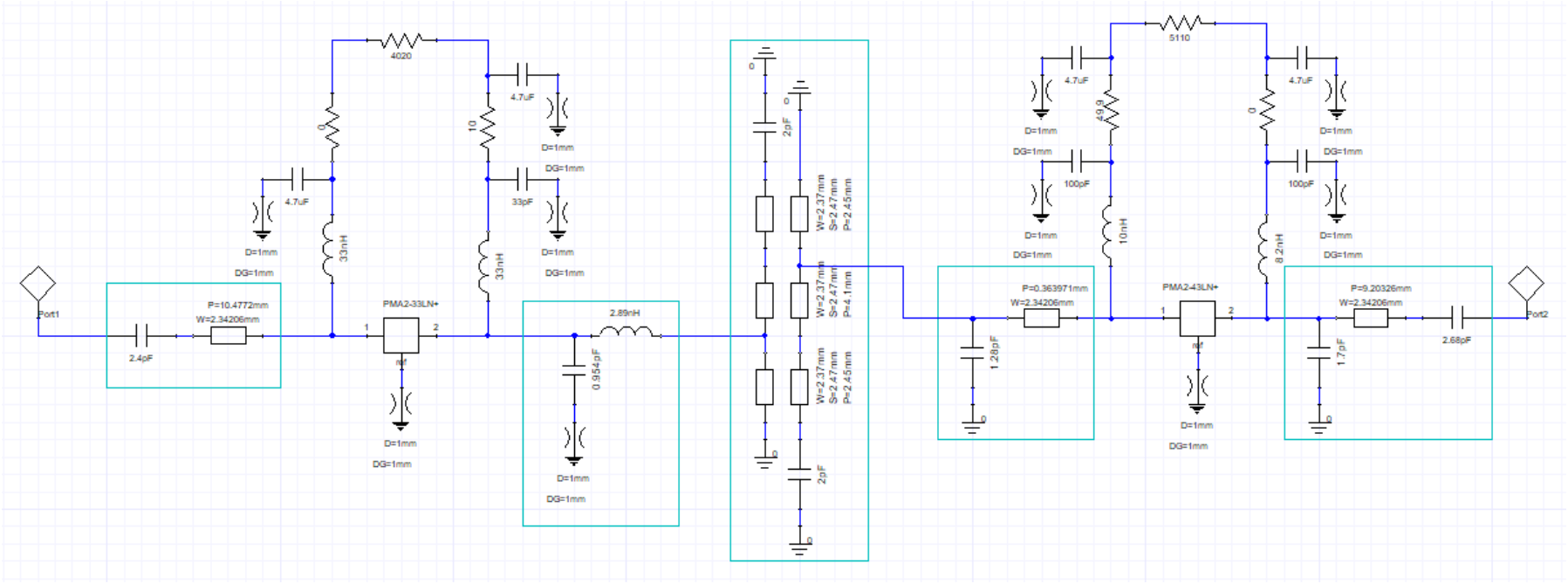

Figure 2.25 Scheme of the LNA with 2 stages and band pass filter.

Figure 2.26 shows the Scattering parameters, the S_{21} parameter has a gain equal to 30.03 dB, and the S_{11} parameter (reflection coefficient) is equal to -9.50 dB at the center frequency of 2.35 GHz.

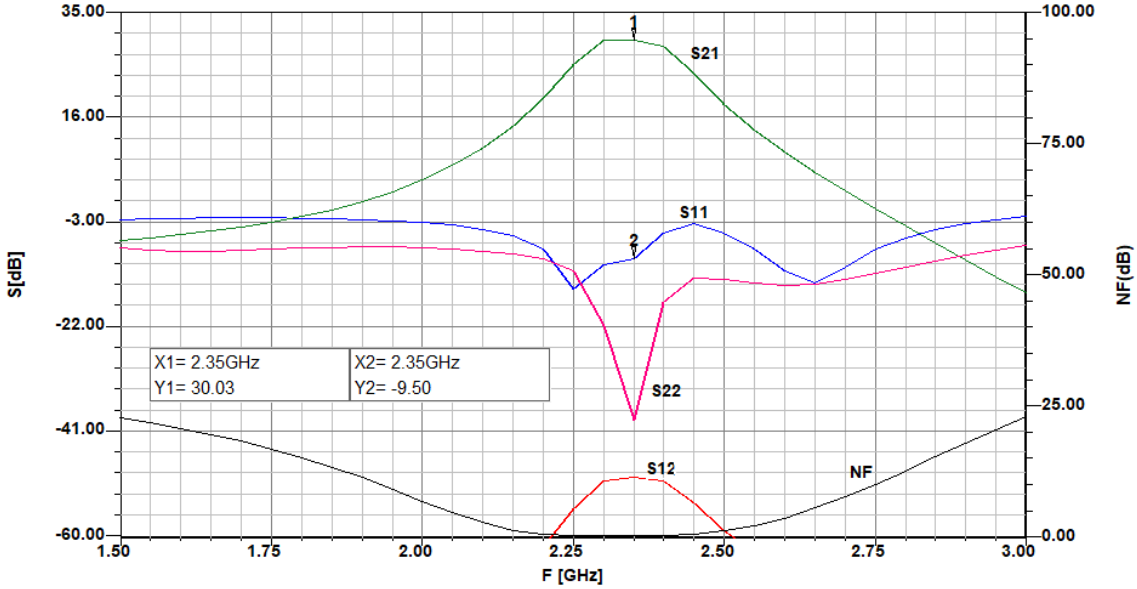

Figure 2.26 S-parameters of the LNA at the frequency range from 1.5 GHz to 3 GHz.

Figure 2.27 shows the value of the noise figure (NF) and the value of the minimum noise figure (F_{min}) at the center frequency of 2.35 GHz equal to 0.41 dB.

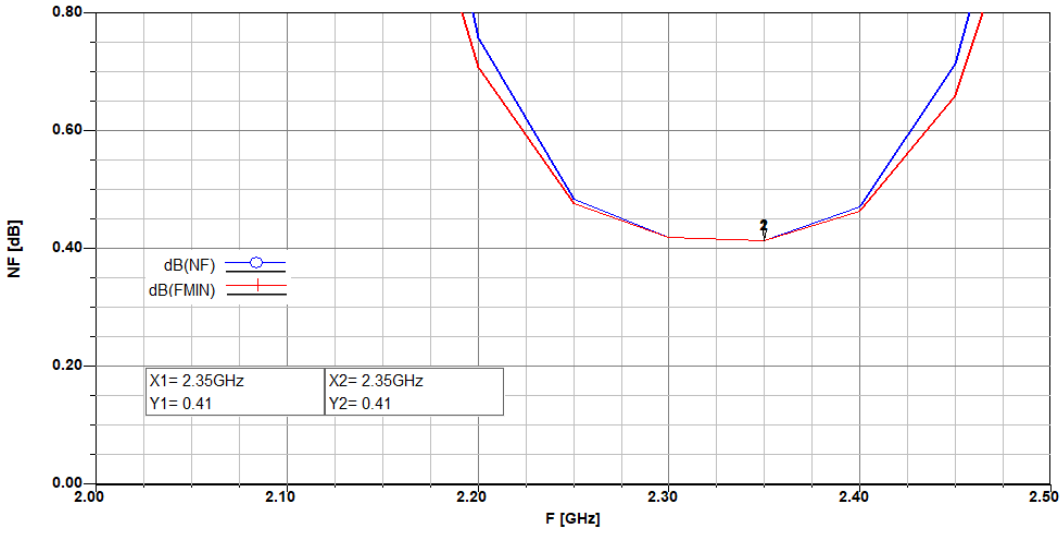

Figure 2.27 Noise figure (NF) and minimum noise figure (F_{min}).

2.6 Design 2 and Simulation of LNA

As stated before, the ATF-54143 amplifier produced by Avago company was chosen as main active device for this second LNA designing. This amplifier has been used in first and second stage of the LNA because of its appropriate characteristics such a low noise figure and high power in the frequency range from 2.3 GHz to 2.4 GHz, which is required in the input and output of this LNA design.

2.6.1 Stage 1 of LNA (ATF-54143)

2.6.1.1 Operating Point and Bias Circuit

The operating point and the bias circuit were chosen based on the manufacturer's recommendation [20]. The operating point values are V_{ds} = 3 V and I_{ds} = 60 mA; and the bias circuit scheme with its respective values is shown in Figure 2.28 and Table 2.4.

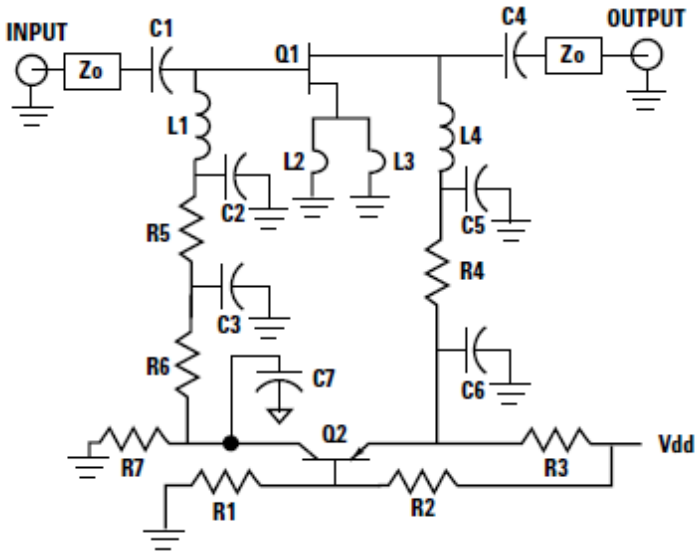

Figure 2.28 Typical ATF-54143 LNA with active biasing [20].

Table 2.4 Component values for manufacture's recommended application [20].

Component	Value
R1	1450 Ω
R2	1050 Ω
R3	23.3 Ω
R4	10 Ω
R5	47 Ω
R6	10 kΩ
R7	1 kΩ
C3, C6, C7	0.01 uF
C1, C4	100 pF
C2, C5	10 pF

2.6.1.2 Amplifier Stability

Just like in the first design of LNA, Ansoft Designer program is used for studying and enhancing the ATF-54143 amplifier stability. Therefore, different graphs and schemes are observed as well, such as the Scattering parameters, the Rollett's stability factor (K) and stability circles on the Smith chart.

Figure 2.29 illustrates the basic schema of the ATF-54143 amplifier stability in Ansoft Designer, which is analyzed independently without other components.

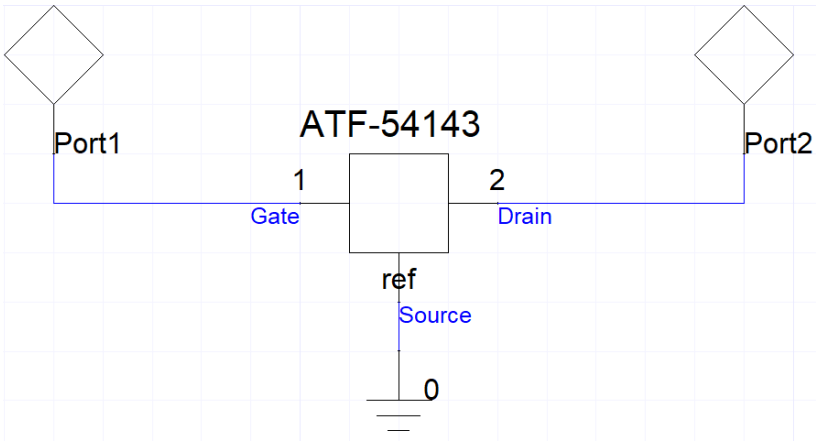

Figure 2.29 ATF-54143 Amplifier – Avago VF JFET Transistor GaAs.

Figure 2.30 shows the Rollett's stability factor (K), as was previously mentioned, it indicates the stability of the transistor for values greater than 1. In this case, it is observed that transistor is not stable throughout the working frequency range of the amplifier, from 0.1 GHz to 18 GHz.

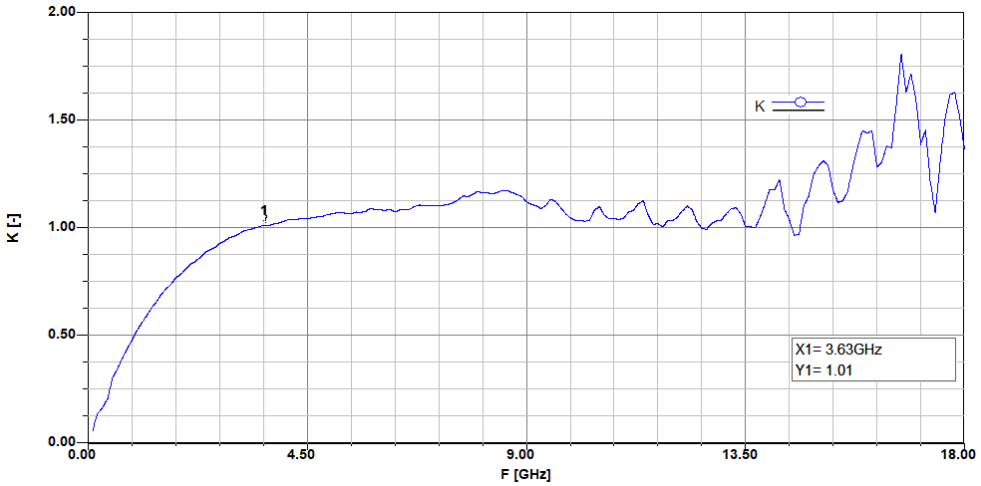

Figure 2.30 Rollett's stability factor (K) – Non stable amplifier in low frequencies.

Figure 2.31 depicts the KCS and KCL stability circles on the Smith chart. It is evident that the amplifier is not stable because both circles KCS and KCL are inside of the Smith chart.

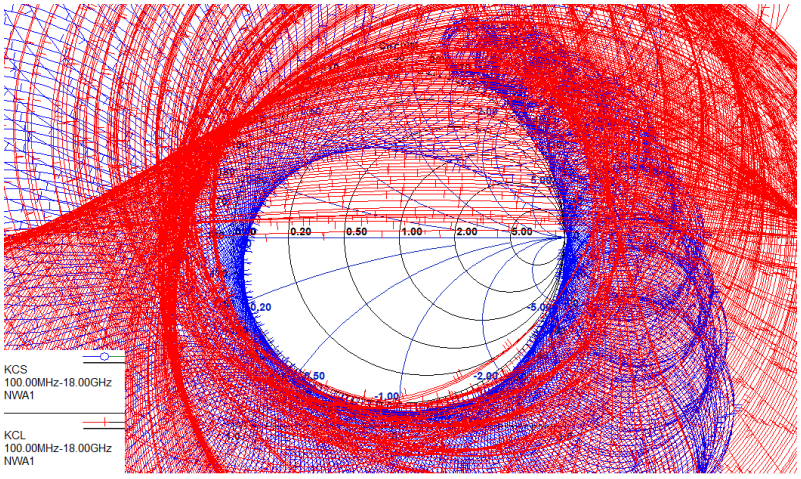

Figure 2.31 KCS and KCL stability circles on the Smith chart – Non stable amplifier.

In order to improve the stability of the transistor, a resistor in series of low value was connected to the drain of the transistor. Taking into consideration the simulation results, the resistor value of 27 Ω has been chosen because this value does not change the behavior of Scattering parameters at given frequency range.

Moreover, very short transmission lines between each source lead and ground have been used, in this manner the stability has improved without much degeneration of the noise properties. These transmission lines now serve as "negative current feedback" and improve the stability. It has been simulated with the following parameters: length P = 1 mm and width W = 0.3 mm, as it is shown in Figure 2.32.

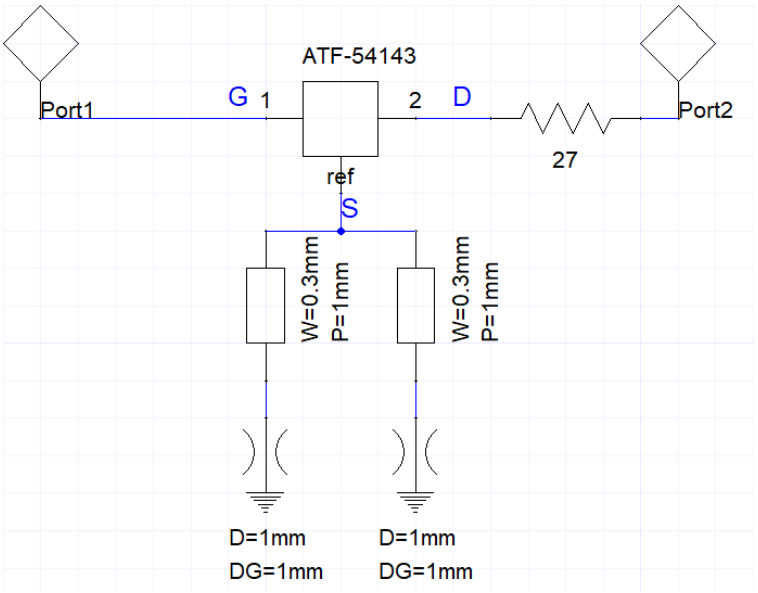

Figure 2.32 Improving the stability of the ATF-54143 transistor.

Figure 2.33 shows the improving stability of the ATF-54143 transistor, but at frequencies below 0.93GHz the amplifier is still unstable.

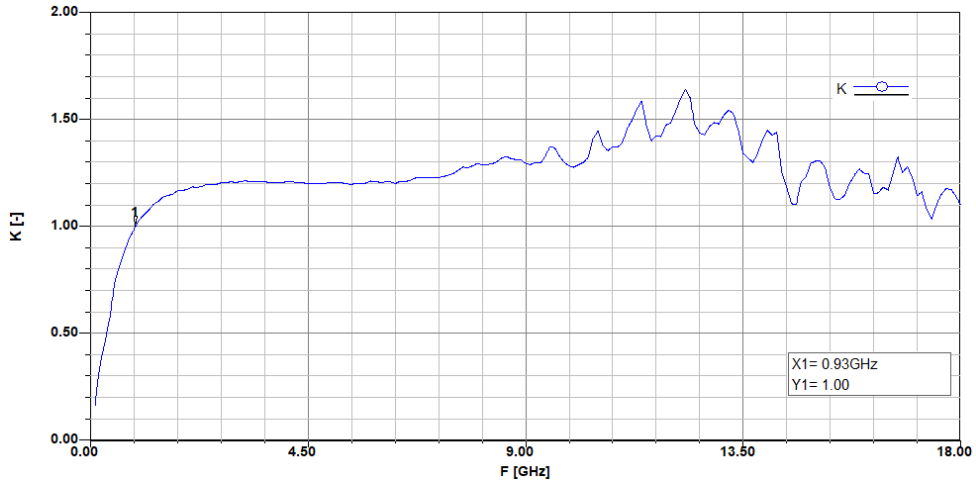

Figure 2.33 Improving stability – Rollett's stability factor (K).

Figure 2.34 illustrates the connection of biasing networks of the ATF-54143 amplifier recommended by Avago Technologies. These networks also influence the stability of the amplifier. The component values were provided by Avago Technologies and some of them were changed in order to improve the performance of the LNA design.

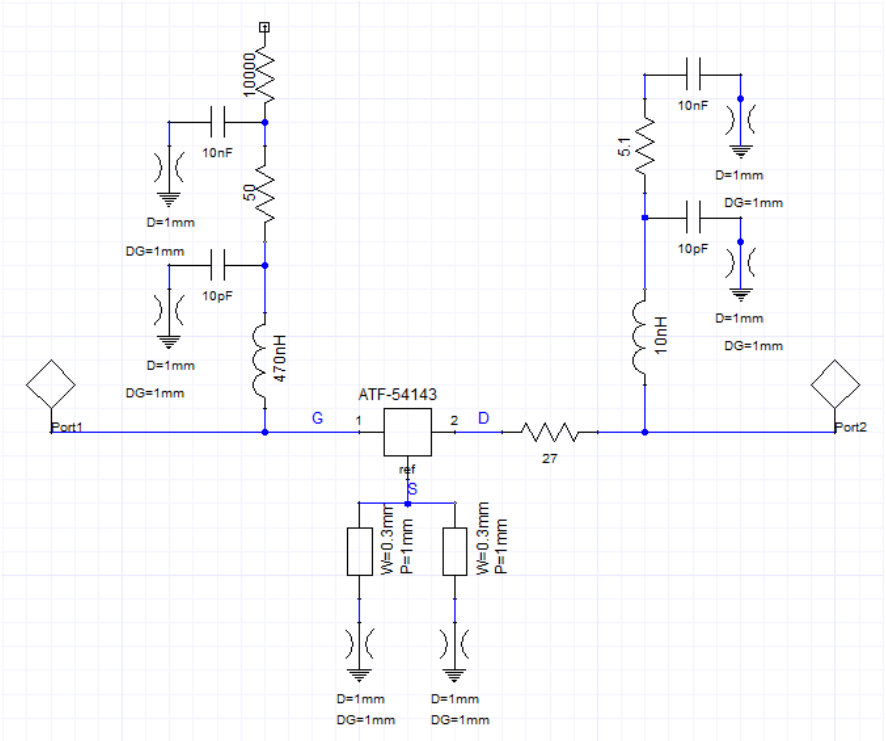

Figure 2.34 Scheme of the ATF-54143 transistor's stability with recommended bias circuit by Avago.

Figure 2.35 shows the complete stability of the amplifier by Rollet stability factor (K), where the amplifier is stable throughout the working frequency range from 0.1 GHz to 18 GHz, and the center frequency of 2.35 GHz is included.

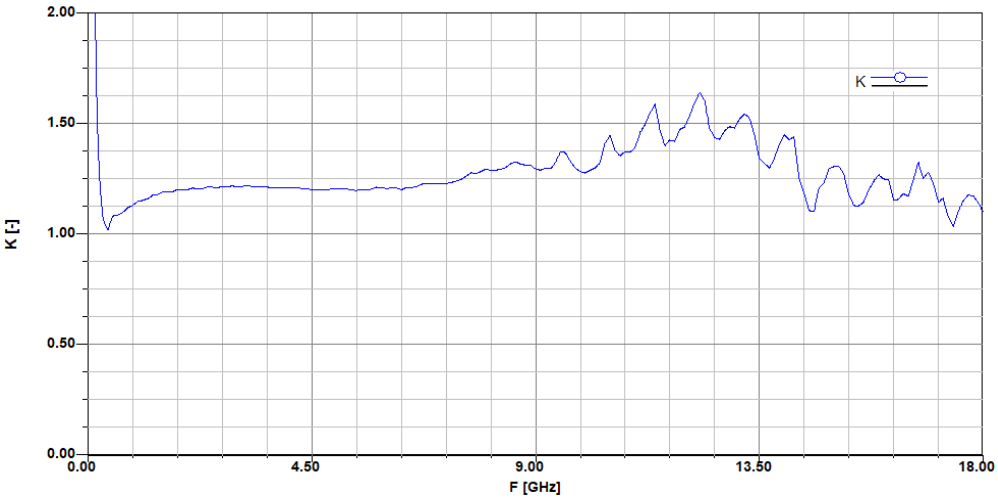

Figure 2.35 Rollett's stability factor (K) – Stable amplifier.

It is also possible to observe the amplifier stability by the stability circles on the Smith chart as seen in Figure 2.36, in this case at the frequency range from 2 GHz to 3 GHz. The KCS and KCL stability circles are outside of the Smith chart, which are the conditions for the stability of the amplifier.

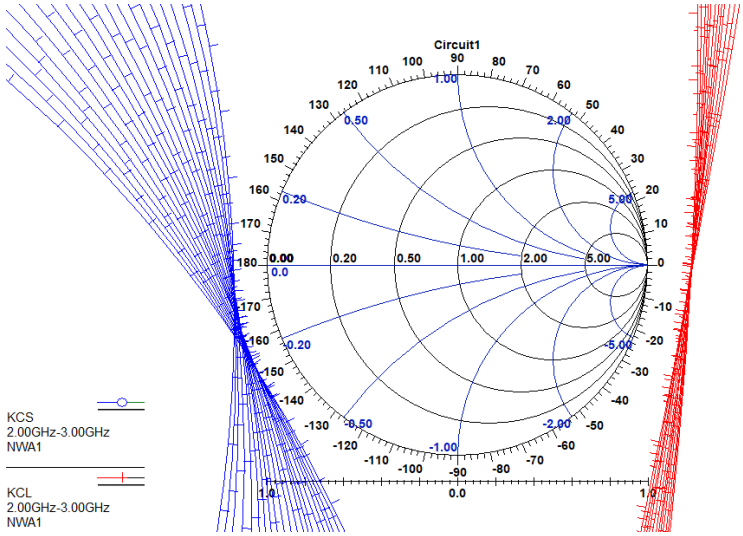

Figure 2.36 KCS and KCL stability circles on the Smith chart at the frequency range from 2 GHz to 3 GHz - Stable amplifier.

2.6.1.3 Impedance Matching Networks

As in the case of the first design of the LNA, the tool known as “Smith Tool” was used. This tool is provided by Ansoft Designer program for finding the impedance matching networks.

To achieve the input impedance matching with impedance of 50 Ω, it was necessary to set the central operating frequency of the LNA at 2.35 GHz. Afterwards, the noise parameter was selected with reference value of minimum noise figure (F_{min}) equal to 0.57 dB.

The next step was to select the Available Gain Circle for Source (GACS) with reference value less than the maximum gain, the reference value selected was equal to 13.98 dB. In this way, the circles of noise and GACS were obtained on the Smith chart. The value of GACS was set in order to obtain an intersection between the circle of GACS and the center of the circle of the noise, the value set was 13.33 dB.

Subsequently, it was possible to choose the suitable components for the input impedance matching, taking into account the center point of the Smith chart and the intersection between the circle of GACS and the center point of the circle of noise as the beginning and final of the selection of components respectively. The result of the steps mentioned can be observed on the Smith chart in Figure 2.37.

The input impedance matching obtained was an inductor equal to 4.36 nH connected in series to a capacitor equal to 3.26 pF. At the same time, this inductor is connected in parallel to input of this LNA stage, it can be observed in Figure 2.39.

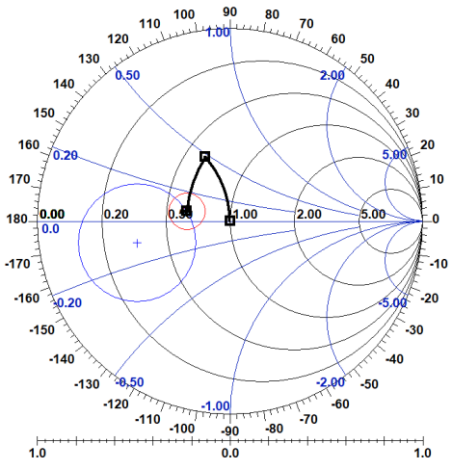

Figure 2.37 Smith Tool – Input impedance matching.

To achieve the output impedance matching with impedance of 50 Ω, same steps were executed as previously for the input impedance matching, but a new configuration was added for obtaining the Available Gain Circle for Load (GACL), which had the same reference value as the GACS (equal to 13.33 dB).

After obtaining the GACL, it was necessary to select the intersection between the GACS circle and the center point of the circle of noise in order to obtain a reference point into the GACL circle. Finally, after these steps, it was possible to obtain the conjugation (marker point) of the previous point obtained from the GACL circle.

This new point was the initial reference for the suitable components chosen for the output impedance matching and the middle of the Smith chart was the final reference. The result of the steps mentioned can be observed on the Smith chart in Figure 2.38.

The output impedance matching obtained was an inductor equal to 2.45 nH connected in series to a microstrip line with length P = 11.60 mm and width W = 2.34 mm as it is shown in Figure 2.39.

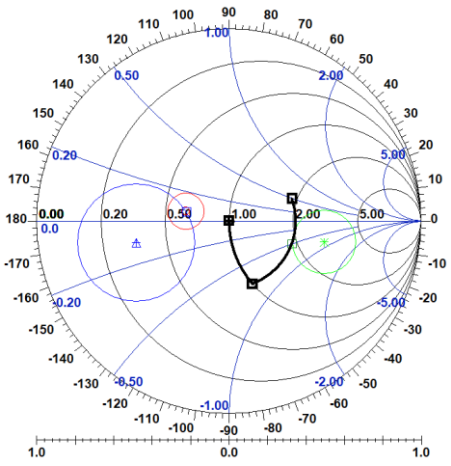

Figure 2.38 Smith Tool – Output impedance matching.

Figure 2.39 shows the scheme of first stage of the LNA, with respectively impedance matching networks obtained for the input and output.

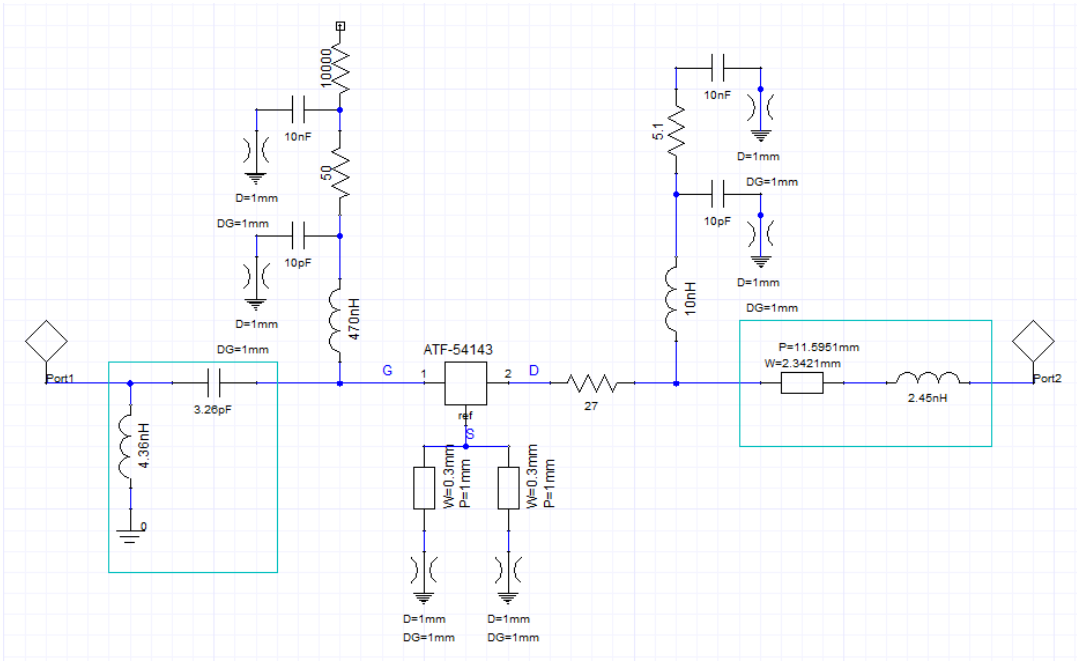

Figure 2.39 Scheme of the first stage of LNA with impedance matching networks for input and output.

Figure 2.40 illustrates the value of the noise figure (NF) and the value of the minimum noise figure (F_{min}) for the LNA at the center frequency of 2.35 GHz after setting the impedance matching networks. It can be observed that value of the noise figure is equal to the value of the minimum noise figure: $\mathrm{NF} = \mathrm{F_{min}} = 0.57$ dB, which indicates that the impedance matching networks were properly designed.

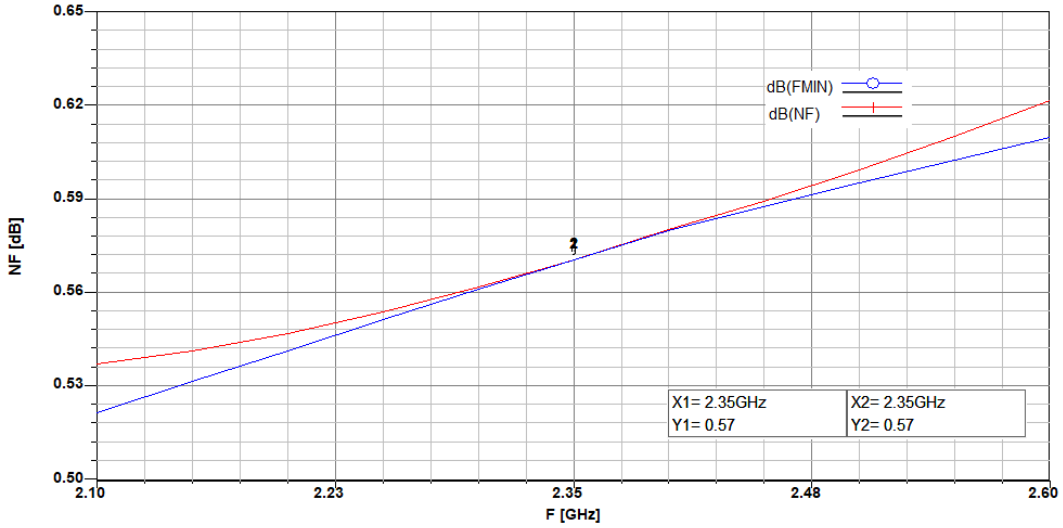

Figure 2.40 Noise figure (NF) and minimum noise figure (F_{min}) with matching networks.

Figure 2.41 depicts the Scattering parameters of the LNA at the center frequency of 2.35 GHz, where the gain obtained is equal to 13.33 dB (S_{21} parameter).

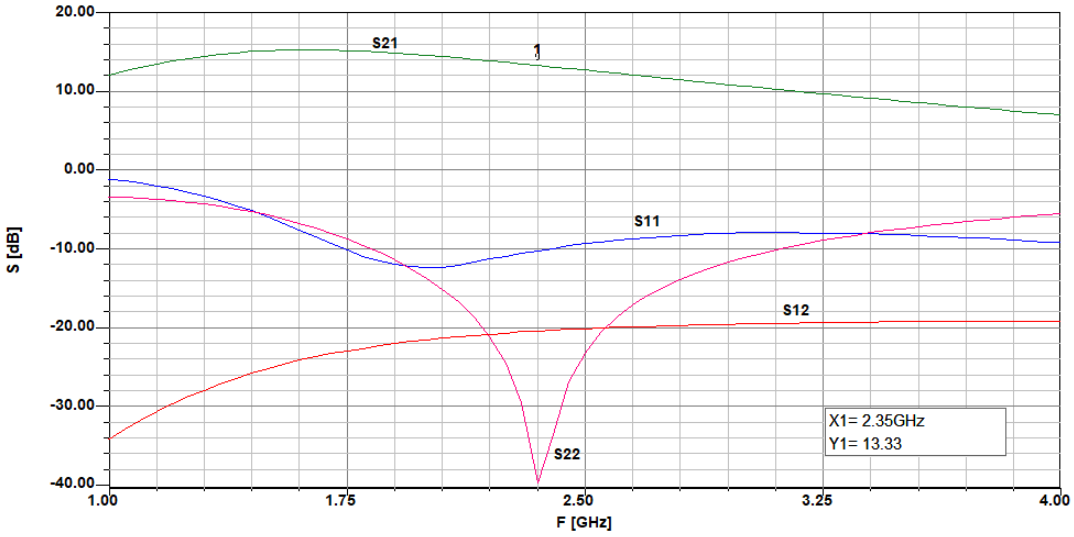

Figure 2.41 S-parameters of the first stage at the frequency range from 1 GHz to 4 GHz.

2.6.2 Stage 2 of LNA (ATF-54143)

All previous steps realized in the first stage of this second LNA design are the same for the second stage, because this stage uses the same ATF-54143 amplifier, with the exception of the impedance matching networks design, which is explained in next section.

2.6.2.1 Impedance Matching Networks

In order to obtain the impedance matching networks, the same steps are performed as in Section 2.5.2.3 of the second stage of the first LNA design. The suitable components for the input and output impedance matching on the Smith chart are shown in Figure 2.42.

The input impedance matching network obtained was a capacitor equal to 2.16 pF

connected in series to an inductor equal to 1.16 nH. At the same time, this capacitor was connected in parallel to the input of this second stage of LNA, which can be observed in Figure 2.43.

The output impedance matching network obtained was a capacitor equal to 0.76 pF connected in series to an inductor equal to 5 nH. This capacitor was also connected in parallel to the output of the ATF-54143 amplifier. The complete connection of the input and output impedance matching networks is shown in Figure 2.43.

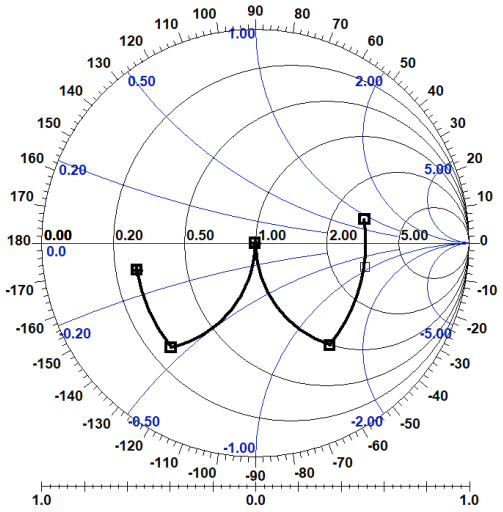

Figure 2.42 Smith Tool – Input and output impedance matching.

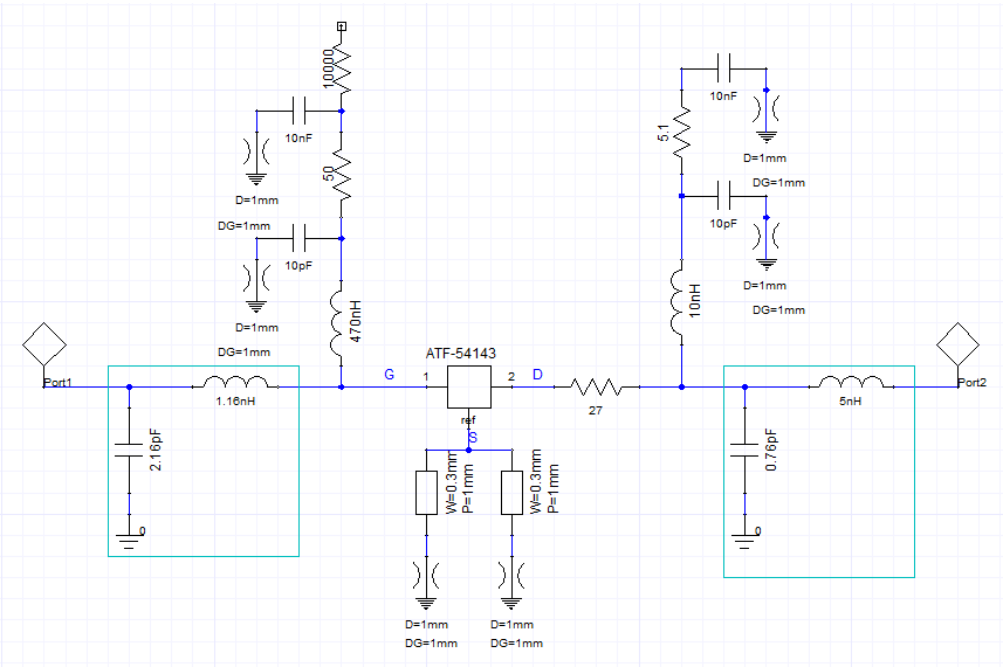

Figure 2.43 Scheme of the second stage of LNA with impedance matching networks for the input and the output.

Figure 2.44 shows the Scattering parameters of the LNA at the center frequency of 2.35 GHz, where the gain obtained is equal to 13.98 dB (S_{21} parameter).

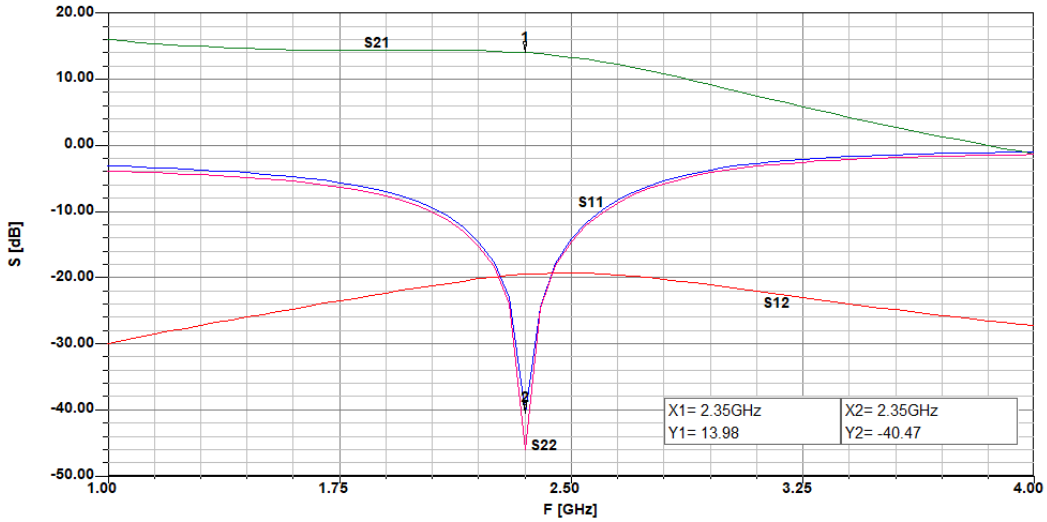

Figure 2.44 S-parameters of the second stage at the frequency range from 1 GHz to 4 GHz.

2.6.3 LNA Results with Band Pass Filter

Figure 2.45 displays the scheme of the LNA design with two stages and microstrip interdigital band pass filter in the middle of these stages.

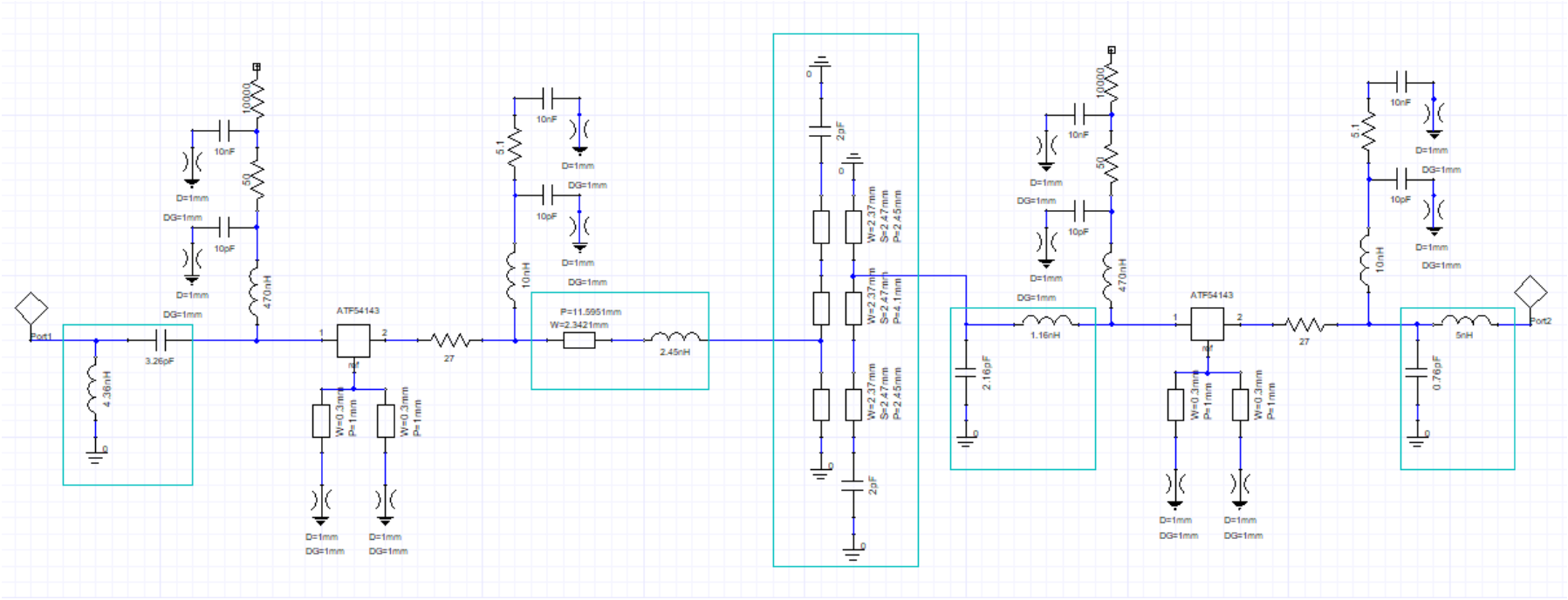

Figure 2.45 Scheme of the LNA with 2 stages and band pass filter.

Figure 2.46 shows the Scattering parameters, the S_{21} parameter has a gain equal to 27.03 dB, and the S_{11} parameter (reflection coefficient) is equal to -9.77 dB at the center frequency of 2.35 GHz.

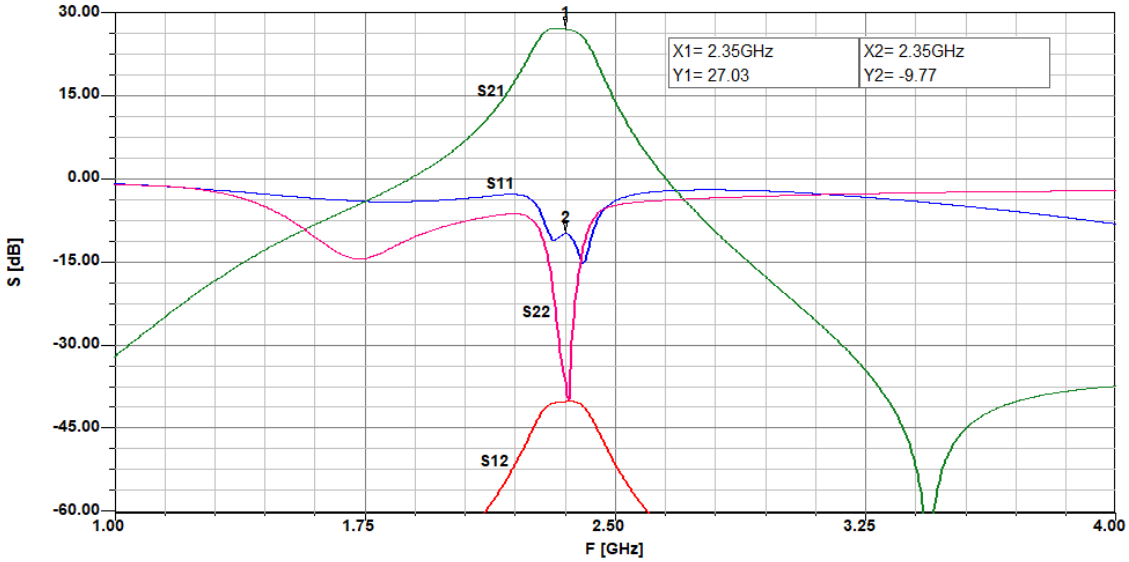

Figure 2.46 S-parameters of the LNA at the frequency range from 1 GHz to 4 GHz.

Figure 2.47 shows the value of the noise figure (NF) and the value of the minimum noise figure (F_{min}) at the center frequency of 2.35 GHz equal to 0.62 dB.

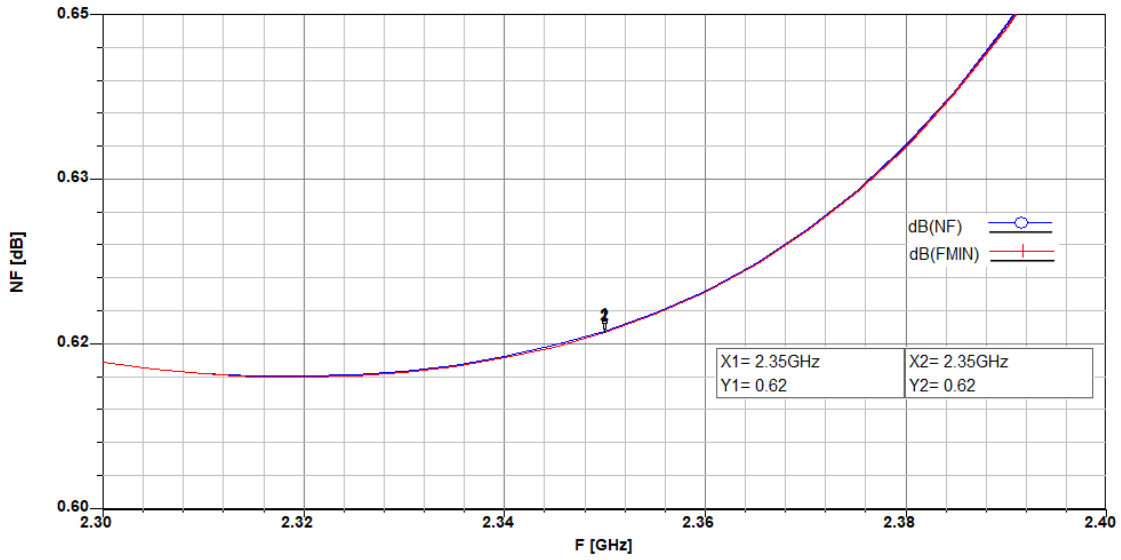

Figure 2.47 Noise figure (NF) and minimum noise figure (F_{min}).

2.7 Comparison of Simulation Results of the LNA Designs

The simulation results of the two proposed designs can be seen in Table 2.2. The design 1 has better results than design 2, such as minor noise and higher gain. Therefore, the design 1 has been proposed for the final realization.

Table 2.5 Simulation results of the LNA with 2 stages and band pass filter for the S band in Ansoft Designer program.

	DESIGN 1	**DESIGN 2**
Amplifier	PMA2-33LN+	ATF-54143
	PMA2-43LN+	
fo [GHz]	2.35	2.35
NF [dB]	0.41	0.62
G [dB]	30.03	27.03
IP3 [dBm]	38.54	36.2
1dB [dBm]	19.11	20.4
BW [MHz]	150	160
Material	SnAgNi E-PHEMT	E-PHEMT GaAs
Producer	Mini-Circuits	Avago

2.8 Low Noise Amplifier Design with Cavity Resonator

As it was mentioned in Section 2.7, the first design of LNA with monolithic amplifiers produced by Mini-Circuits have been chosen for realization of this work. In order to simulate the complete LNA was necessary to export the Scattering parameters of the cavity resonator from HFSS program to Ansoft Designer program in Touchtone file format.

Figure 2.48 shows the complete scheme of the LNA with 2 stages, the microstrip interdigital band pass filter, and the coaxial cavity resonator in the input.

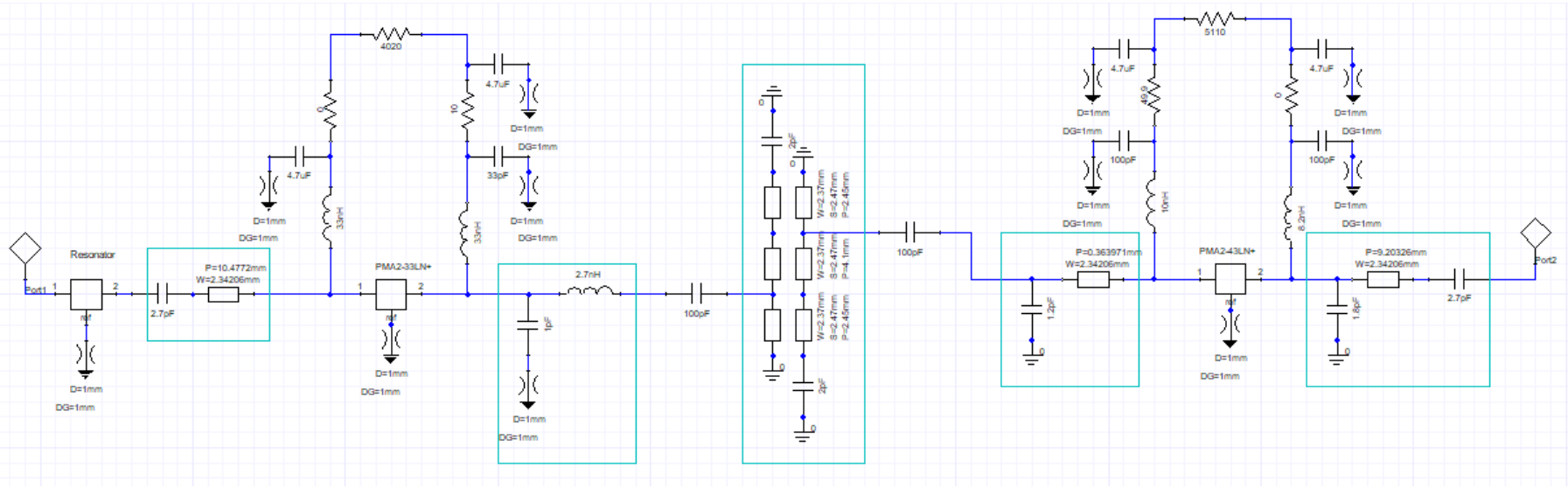

Figure 2.48 Complete scheme of the LNA with the band pass filter and the cavity resonator in the input.

Figure 2.49 shows the simulation of the complete LNA, where the gain is equal to 30.02 dB, the noise figure is equal to 0.48 dB and the bandwidth of approximate value equal to 180 MHz (-3 dB cutoff frequency), all of them at the center frequency of 2.35 GHz.

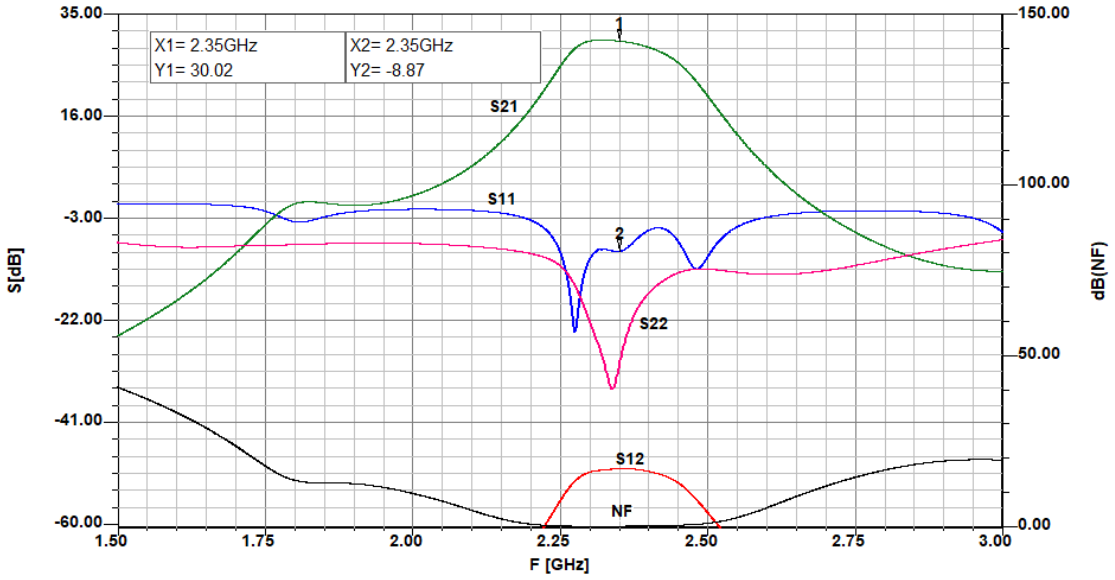

Figure 2.49 S-parameters of the LNA design at the center frequency of 2.35 GHz.

Figure 2.50 illustrates a block diagram of the complete LNA design with the microstrip interdigital band pass filter and the coaxial cavity resonator in the input.

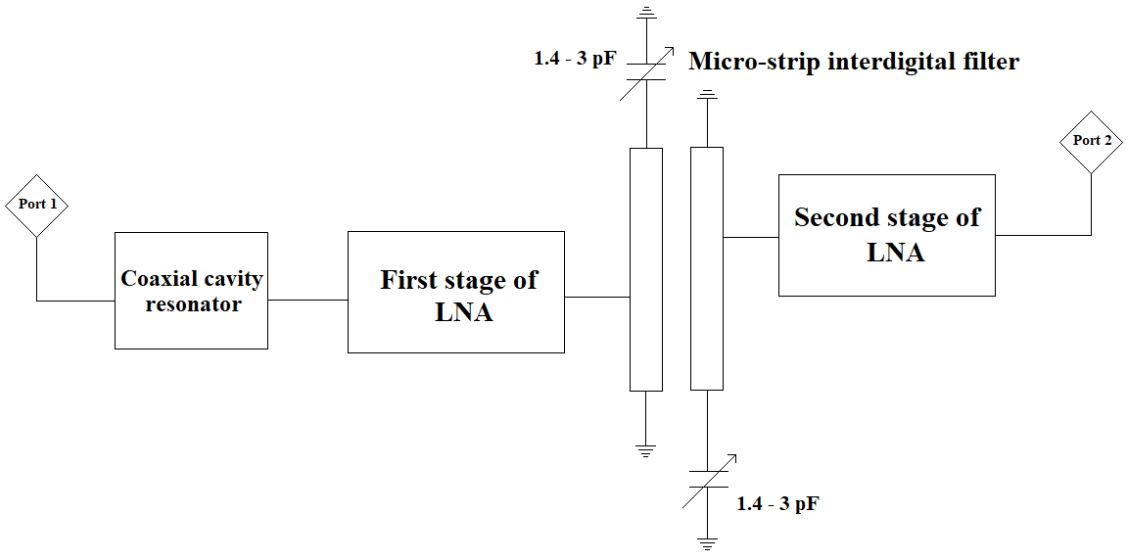

Figure 2.50 Block diagram of the complete LNA design with the coaxial cavity resonator.

2.9 Realization and Measurement Results of the LNA

2.9.1 Realization of the LNA

For the fabrication of the Printed Circuit Board (PCB) of the LNA was used the EAGLE PCB design software version 7.6.0. The choice of this software as a designing tool for the PCB of the LNA was made due to its flexibility in its capabilities, workflow compatibility, extensive fully-open component library to work as well as its rich variety of tools and also due to its simplicity to use.

In the design of this LNA, the appropriate distribution of the spaces for the components on the PCB has been considered. The location of the PMA2-33LN+ monolithic amplifier was defined carefully in order to obtain the lowest possible noise figure. For example, the shortest possible distance between the components of the input impedance matching network (first stage of LNA) and the RF input pin of the PMA2-33LN+ monolithic amplifier has been considered during the design. The final design of the PCB with its real dimensions such as width 56 mm, length 68 mm and height 0.79 mm can be observed in Attachment B.1.

As previously mentioned, the material used for the PCB was Arlon CuClad 217 substrate, which was provided by the Faculty of Electrical Engineering and Communication of Brno University of Technology. The principal advantage of this material is its good performance in radio frequency signals, which is suitable for this LNA design due to its work frequency in the S band.

After the fabrication of the PCB previously designed, the next step was its implementation with the electrical components, which have been chosen and calculated for this design. As shown in Figure 2.52, they were carefully soldered on the PCB in order to avoid any damage on them and within the conductor lines of the PCB. On the other hand, as it can be observed in the circuit scheme in the Attachment A, it is important to know that not all the component values used here were ideal, but they were as close as possible.

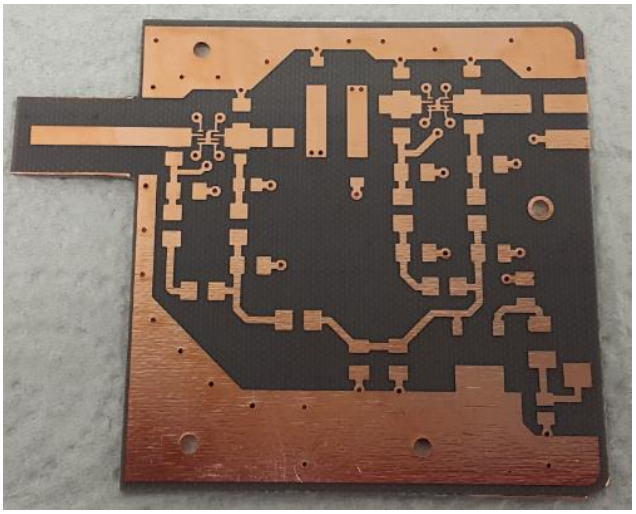

Figure 2.51 Printed circuit board (PCB) of the LNA for the S band.

2.9.2 Realization of the Coaxial Cavity Resonator

For the fabrication of the coaxial cavity resonator a mechanical structure of aluminum was designed and implemented in which the cavity resonator and the PCB will be placed together. The dimensions of the cavity resonator obtained by the ANSYS HFSS program were used for its fabrication. The coaxial cavity resonator consists of an external and internal structure.

The internal structure or internal resonator is made of brass metal because brass has good performance for soldering and the input and output of the cavity resonator will be connected by soldering. The external structure or external resonator has a square shape with the following dimensions: Depth equal to 24 mm, width equal to 24 mm and height equal to 25 mm. The internal resonator has a cylindrical shape with the following dimensions: Height equal to 21.2 mm and diameter equal to 7 mm. This latter internal resonator is fixed in center of the external resonator with a screw M3. The other end of the internal resonator contains a 15 mm deep hole with a diameter of 5mm which is filled with Teflon (PTFE). Along the Teflon is another hole with a diameter of 2.5 mm, in which the screw M2,5 will be displaced for tuning the center frequency of the LNA.

The input of the cavity resonator is connected directly through a SMA connector of 50 Ω impedance from the external resonator to internal resonator and a height equal to 8 mm from the bottom side of the external resonator. The output of the cavity resonator is connected directly from the internal resonator through a ceramic capacitor (part of the input impedance matching) of 2.7 pF to the PCB, and a height equal to 10 mm from the bottom side of the external resonator. A major distance between components in the input of the LNA and the output of cavity resonator generates a major noise, and for this reason the input of the PCB is inside of the external resonator in order to reduce the noise figure in the LNA as can be observed in Figure 2.52.

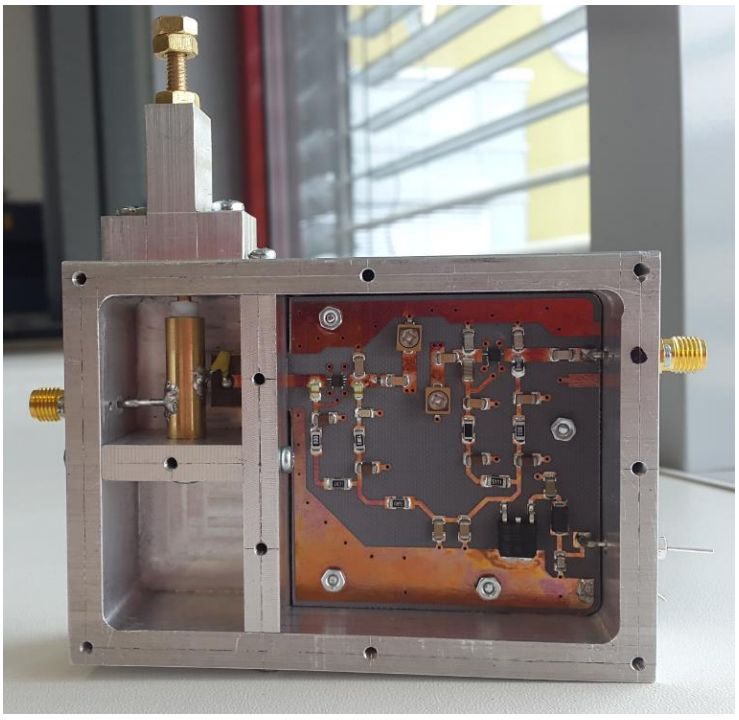

Figure 2.52 LNA for the S band with the coaxial cavity resonator (top side).

Figure 2.53 shows the complete structure closed with its aluminum cover and fixed through M2.5 screws. In fact, the cavity resonator must be completely closed in order to work properly.

Finally, the output of the LNA is connected through another SMA connector of 50 Ω impedance. Also, a pin +12 V connector for the power supply of the LNA was collocated in the structure as can be observed in Figures 2.52 and 2.53. The dimensions of the complete structure are shown in Attachment D.

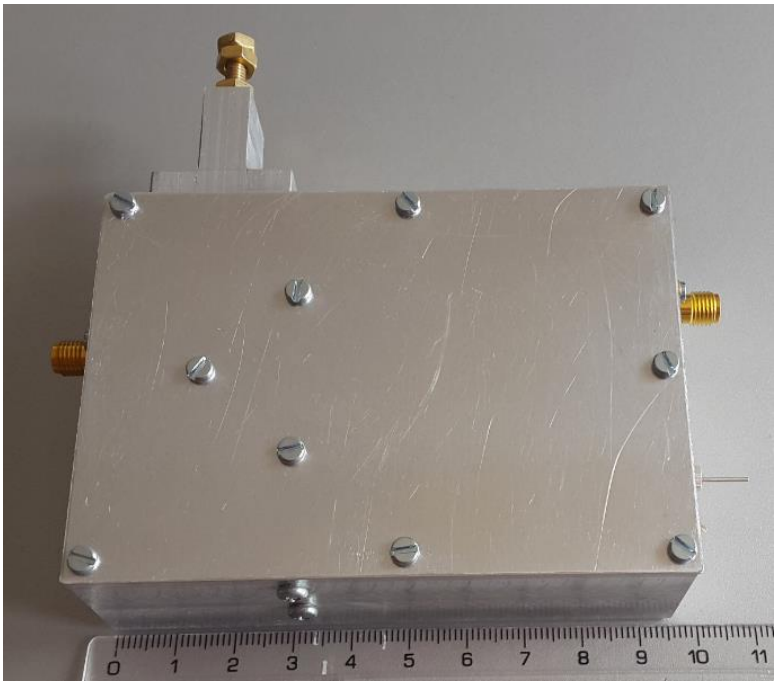

Figure 2.53 LNA for the S band (top side).

2.9.3 Measurement of the Complete LNA

The parameters of the complete LNA for the S band from 2.3 GHz to 2.4 GHz were measured twice. For the first measurement, the Rohde & Schwarz-FSL spectrum analyzer (9 kHz – 3 GHz) and the Agilent-signal generator (9 kHz – 3 GHz) were used. An amplitude signal equal to -40 dBm at the frequency 2.35 GHz from the signal generator to input of the LNA was introduced, and then the output signal of the LNA equal to -22.63 dBm was observed in the spectrum analyzer. Therefore, the gain (S_{21} parameter) of the LNA was 17.37 dB at the frequency of 2.35 GHz. This value of gain was a reference value because it could not be possible to measure other parameters such as the noise figure and reflection coefficients with these instruments. For these parameters, it was necessary to make another measurement.

For the second measurement the Rohde & Schwarz-FSP Scalar spectrum analyzer was used. All S-parameters were observed in this measurement, where the gain (S_{21} parameter) was equal to 10 dB. It was also observed that this gain was being attenuated by the reflection coefficients (S_{22}, S_{11}), which generate oscillations in the working frequency of this LNA design. For this reason, different values of gain were generated in

the first and second measurements. In the following part (Conclusion), the possible causes of this instability in the LNA and the possible solutions are explained.

Figure 2.54 shows the first measurement process with instruments provided by the department of Radio Electronics-FEKT.

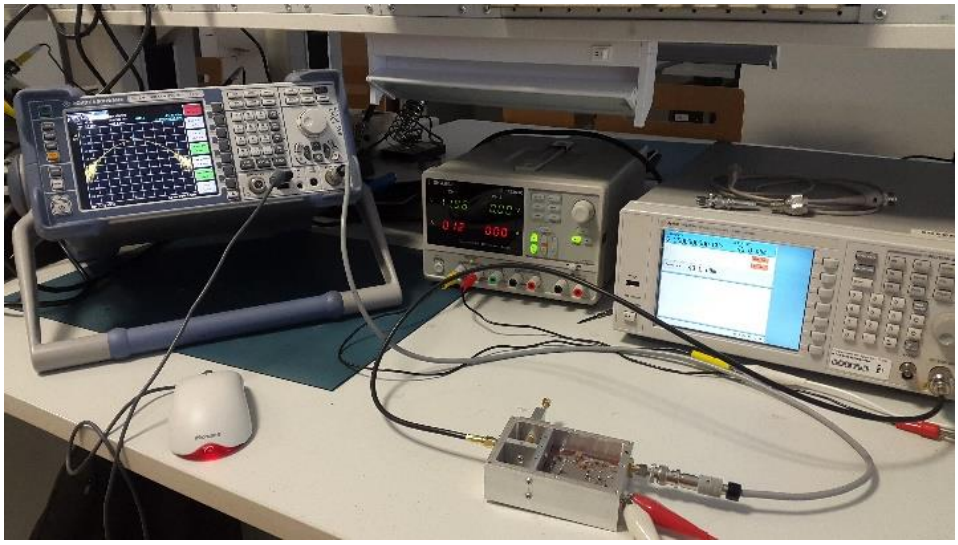

Figure 2.54 First measurement of the LNA.

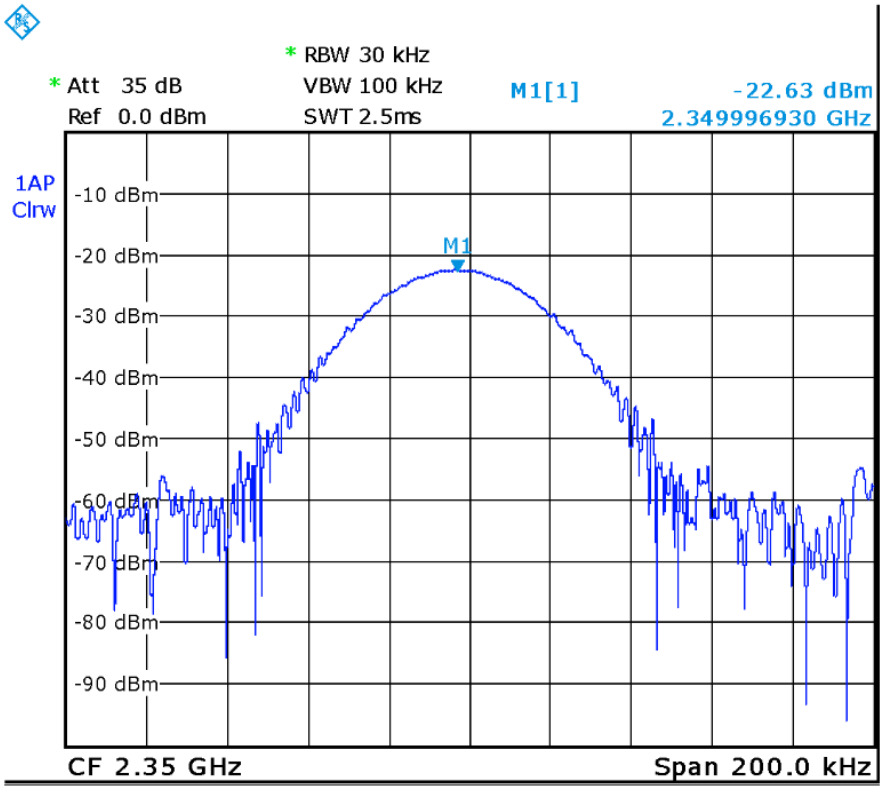

Figure 2.55 Gain of the first measurement.

3 CONCLUSION

The master's thesis presented the design of a low noise amplifier (LNA) for S band from 2.3 GHz to 2.4 GHz. The main objectives of this design were to obtain a gain greater than 20 dB, a minimum insertion noise, and input and output impedance of 50 ohms. Very important tools have been used for designing and optimization the LNA, such as the Ansoft Designer program and the HFSS (High Frequency Structure Simulator). This master's thesis is divided in two principal parts. The first part discussed essential characteristics, parameters and concepts for designing a LNA, such as noise figure, scattering parameters, stability, power gain, nonlinearities in amplifiers and impedance matching networks. In Sections 1.3 and 1.4 of this part, fundamental concepts for designing selective circuits were explained, such as microstrip band pass filters and cavity resonators. These fundamentals are key to introducing the concept and mechanism of the present LNA design. The second part was divided in nine sections, where two designs of the LNA with different active devices were proposed. The first design exhibited better simulated results than the second one, as observed in Table 2.5. As a basic part of selectivity of this LNA design a microstrip interdigital band pass filter and a coaxial cavity resonator were proposed as well. Finally, the first LNA design with these selective circuits was optimized, fabricated, and measured.

PMA2-33LN+ and PMA2-43LN+ monolithic amplifiers produced by Mini-Circuit company were used as the main active devices in this LNA design. The results obtained from simulation at the center frequency of 2.35 GHz with selective circuits were: Gain equal to 30.02 dB with bandwidth of approximately 180 MHz (-3 dB cutoff frequency), and noise figure equal to 0.48 dB. The results obtained from measurement at the center frequency of 2.35 GHz did not agree with the simulated values because the LNA is not stable and generates oscillations. Consequently, different values of gain were measured in the LNA such as 10 dB and 17.37 dB. The possible causes of these oscillations could be an imprecision in the design of the PCB layout, where the grounds via connections of monolithic amplifiers must be closer to themselves. Furthermore, another cause could be the two connections under the amplifiers in the bottom side of the PCB layout, where apparently there should not be any connection traces because these monolithic amplifiers are very sensitive, according to the producer.

Taking into account these considerations, it was decided to design, implement and measure a new PCB layout design in order to compare both simulated and new measured property results of the LNA. The new PCB layout was designed and printed as can be observed in Attachments C1 – C3. In addition to this, it was implemented by soldering all the components and mounting in the mechanical structure, as shown in Attachments C.4 and C.5.

As per agreement with the supervisor of the present master’s thesis, the final measured results and the analysis of the LNA properties with the new layout design will be presented in the official presentation term of this work and attached to this master’s thesis.

BIBLIOGRAPHY

[1] *IRE Standards on Methods of Measuring Noise in Linear Twoports, 1959.* Proceedings of the IRE, vol. 48, no. 1, pp. 60-68, January 1960.

[2] POZAR, D. M. *Microwave Engineering*. 4th edition. John Wiley and Sons, Inc., 2011. ISBN 978-0-470-63155-3.

[3] KUROKAWA, K. *Power waves and the scattering matrix*. IEEE Transactions on Microwave Theory and Techniques, vol. 13, no. 2, 1965.

[4] GONZALEZ, G. *Microwave Transistor Amplifiers: Analysis and Design*. 2nd edition. Prentice Hall, Inc., 2008. ISBN 978-9-861-54694-0.

[5] LUDWIG, R., BRETCHKO, P. *RF Circuit Design: Theory and Applications*. 2nd edition. Prentice Hall, Inc., 2000. ISBN 978-0-130-95323-0.

[6] GILMORE, R., BESSER, L. *Practical RF Circuit Design for Modern Wireless Systems, v*ol. 2. Artech House, 2003. ISBN 978-1-580-53522-9.

[7] ROTHE, H., DAHLKE, W. *Theory of noisy Fourpoles.* Proceedings of the IRE, no. 6, pp 811-818, June 1956, vol. 44.

[8] RAZAVI, B. *RF Microelectronics.* 2nd edition. Prentice Hall, Inc., 2011. ISBN 978-0-137-13473-1.

[9] *Accurate and Rapid Measurement of IP2 and IP3.* Analysis, Designer's Guide Consulting, Inc., May 2002.

[10] RAIDA, Z., et al. Multimedia textbook: *Electromagnetic waves, Microwaves technique* [online]. Brno: FEEC BUT Brno, 2010 [cit. 2018-11-10]. Available from URL: http://www.urel.feec.vutbr.cz/~raida/multimedia/index.php.

[11] BALANIS, C. A. *Antenna Theory: Analysis and Design*. 3rd Edition. Hoboken: J. Wiley & Sons, 2005. ISBN 0-471-66782-X.

[12] HANUS, S., SVAČINA, J. *Vysokofrekvenční a mikrovlná technika: přednášky*. V Brně: Vysoké učení technické, Fakulta elektrotechniky a komunikačních technologií, Ústav radioelektroniky, 2002. 208 s.

[13] PETRŽELA, J. *Teorie elektronických obvodů: skripta.* Vyd. 1. V Brně: Vysoké učení technické, Fakulta elektrotechniky a komunikačních technologií, Ústav radioelektroniky, 2012. 200 s. ISBN 978-80-214-4494-2.

[14] GREBENNIKOV, A. *RF and Microwave Transmitter Design*. John Wiley and Sons, Inc., 2011. ISBN 978-0-470-52099-4.

[15] MALORATSKY, L. A. *Passive RF and Microwave Integrated Circuits*. Elsevier Inc., 2004. ISBN 978-0-750-67699-1.

[16] LÁČÍK, J. *Mikrovlná technika: přednášky*. V Brně: Vysoké učení technické, Fakulta elektrotechniky a komunikačních technologií, Ústav radioelektroniky.

[17] ZHANG, K., LI, D. *Electromagnetic Theory for Microwaves and Optoelectronics*. 1st edition, Springer, 1998. ISBN 978-3-662-03555-9.

[18] MINI-CIRCUITS. *PMA2-33LN+: Data Sheet* [online]. [cit. 2018-08-15]. Available from URL:<https://www.minicircuits.com/pdfs/PMA2-33LN+.pdf>.

[19] MINI-CIRCUITS. *PMA2-43LN+: Data Sheet* [online]. [cit. 2018-08-15]. Available from URL:<https://www.minicircuits.com/pdfs/PMA2-43LN+.pdf>.

[20] AVAGO *Technologies. ATF-54143: Data Sheet* [online]. [cit. 2018-08-15]. Available from URL:<https://www.broadcom.com/products/wireless/transistors/fet/atf-54143>.

[21] YOUNES, A., MILLER, F. *Characteristic Impedance of Rectangular Coaxial Transmission Lines.* IEEE, vol. 71, no. 1, pp. 81-89, January 1952.

[22] CYLINDRICAL CAPACITOR CALCULATOR [online]. [cit. 2018-09-20]. Available from URL:< http://hyperphysics.phy-astr.gsu.edu/hbase/electric/capcyl.html#c2>.

INDEX OF SYMBOLS, QUANTITIES AND ABBREVIATIONS

B	Bandwidth [Hz].
DC	Direct Current [A].
F	Noise Factor [-].
F_{min}	Minimum Noise Figure [dB].
f	Frequency [Hz].
G	Gain [dB].
GACS	Available Gain Circle for Source.
GACL	Available Gain Circle for Load.
HFSS	High Frequency Structure Simulator.
K	Rollett's Stability Factor [-].
k	Boltzmann Constant [JK^{-1}].
KCS	K-Factor Circle for Source.
KCL	K-Factor Circle for Load.
LNA	Low Noise Amplifier.
MAG	Maximum Available Gain.
MSG	Maximum Stable Gain.
NF	Noise Figure [dB].
OIP3	Third-Order Output Intercept Point [dBm].
PCB	Printed Circuit Board.
$P\text{-}_{1dB}$	One-dB Output Compression Point Power Level [dBm].
Q	Quality Factor [-].
RF	Radio Frequency.
RL	Return Loss [dB].
SMD	Surface Mount Device.
T	Temperature [K].
T_0	Room Temperature = 290 K.
T_e	Equivalent Noise Temperature [K].
ε_r	Relative Permittivity [-].
λ	Wave-length [m].
Z	Impedance [Ω].

A LNA CIRCUIT DIAGRAM

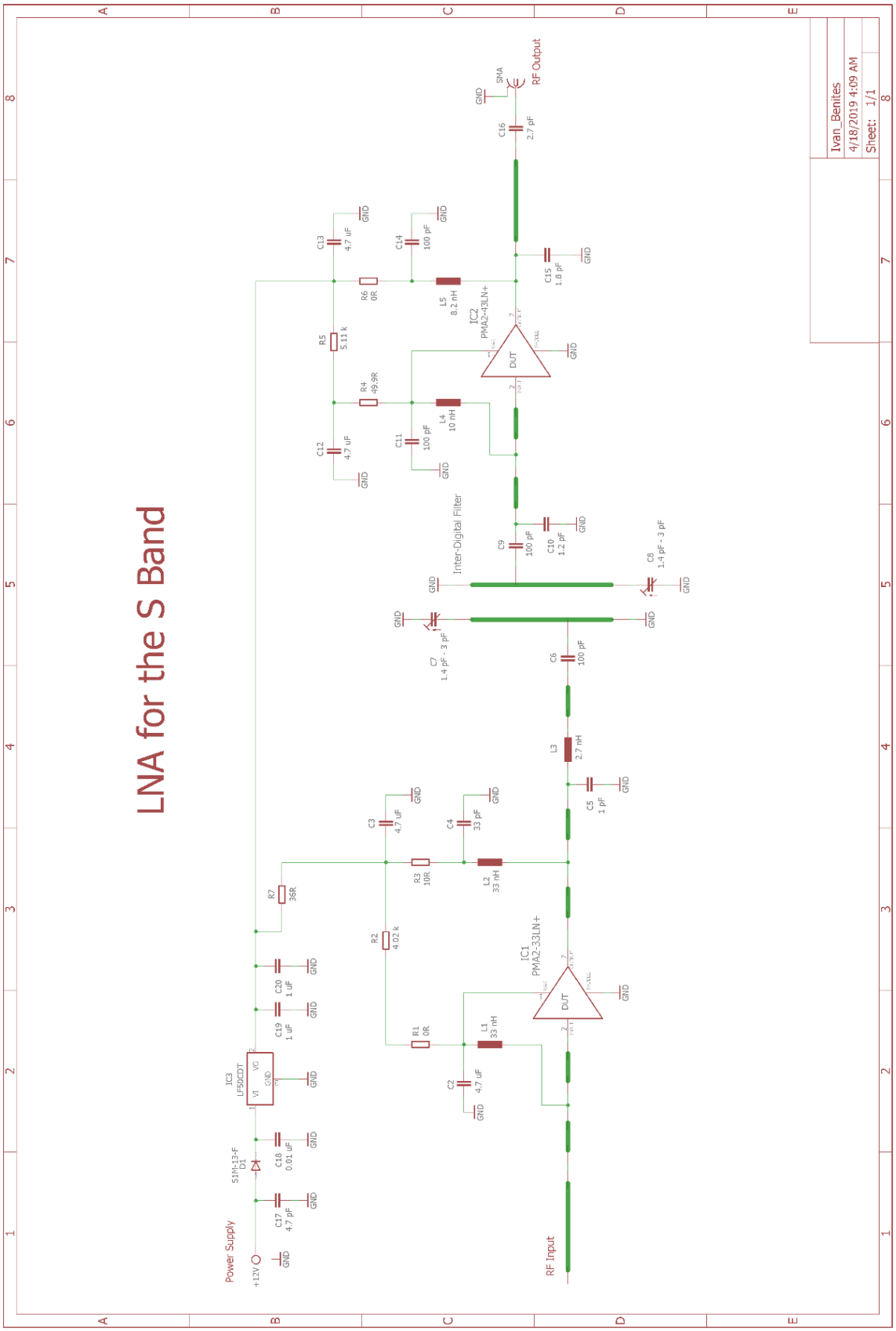

B DESIGN 1 – PCB LAYOUT

B.1 Printed Circuit Board (PCB) – Top (Component lines)

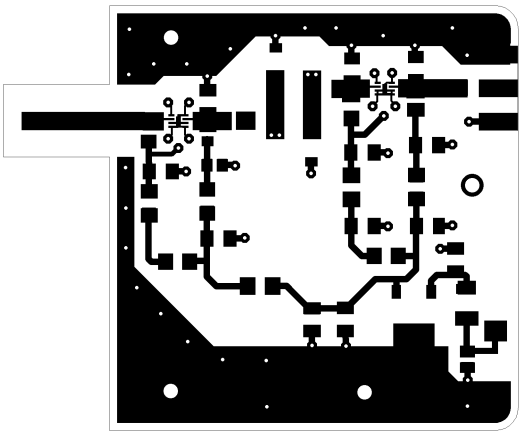

Dimensions of board 56 x 68 [mm], scale M1:1

B.2 Printed Circuit Board (PCB) – Top (Component side)

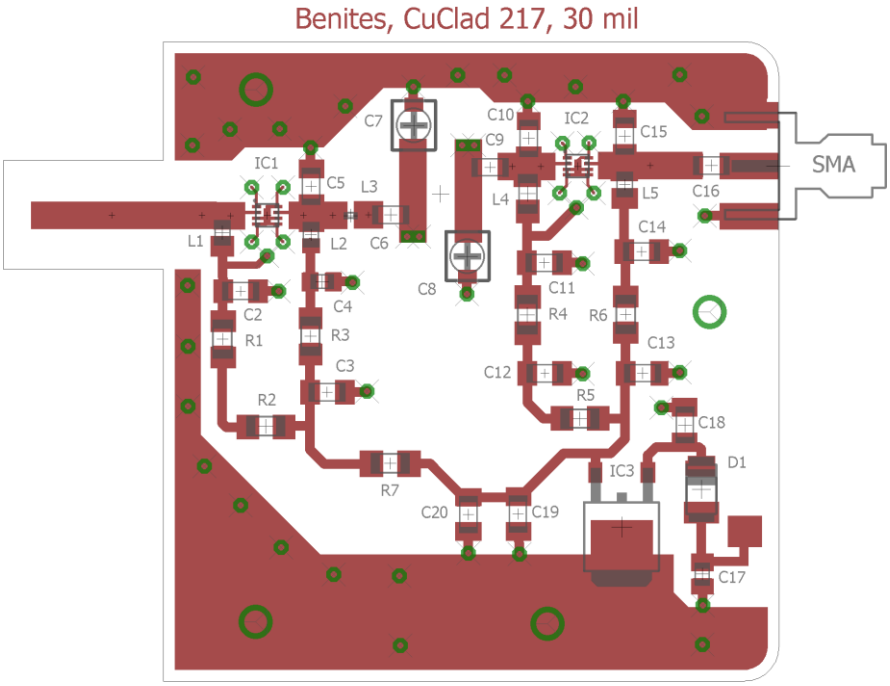

B.3 Printed Circuit Board (PCB) – Bottom (Connection side)

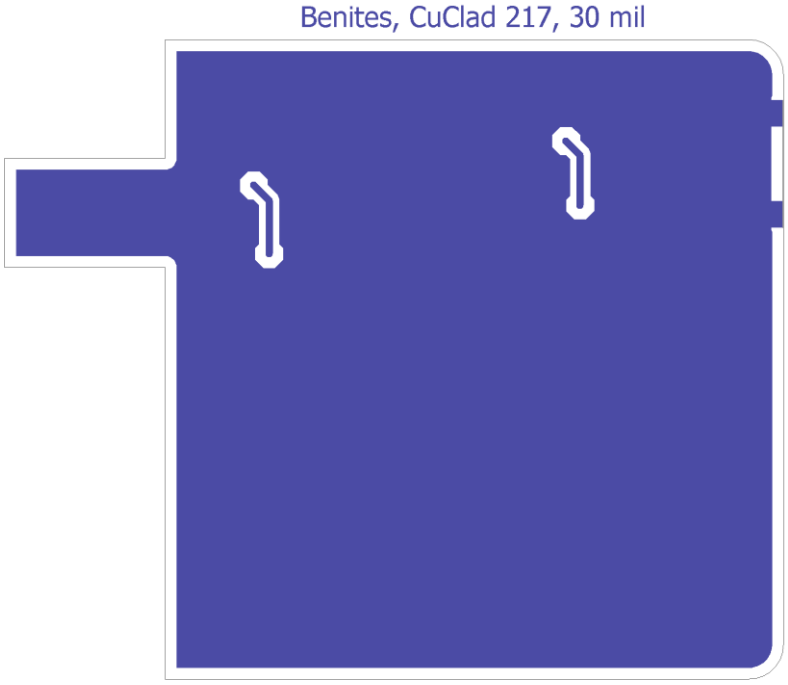

C DESIGN 2 – PCB LAYOUT

C.1 Printed Circuit Board (PCB) – Top (Component lines)

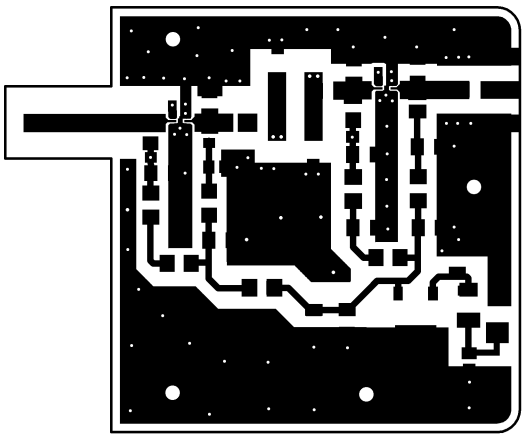

Dimensions of board 56 x 68 [mm], scale M1:1

C.2 Printed Circuit Board (PCB) – Top (Component side)

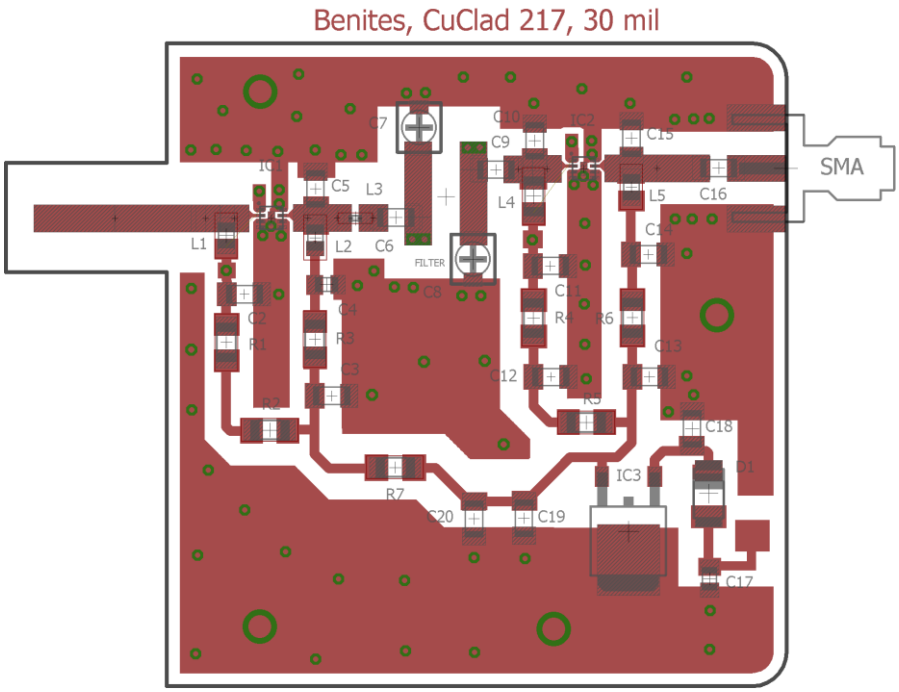

C.3 Printed Circuit Board (PCB) – Bottom (Connection side)

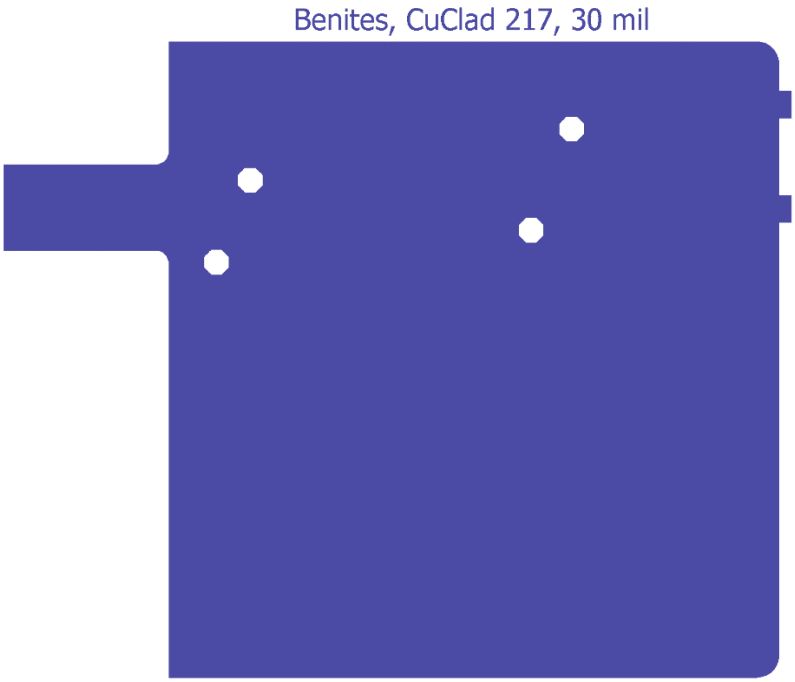

C.4 PCB Implementation

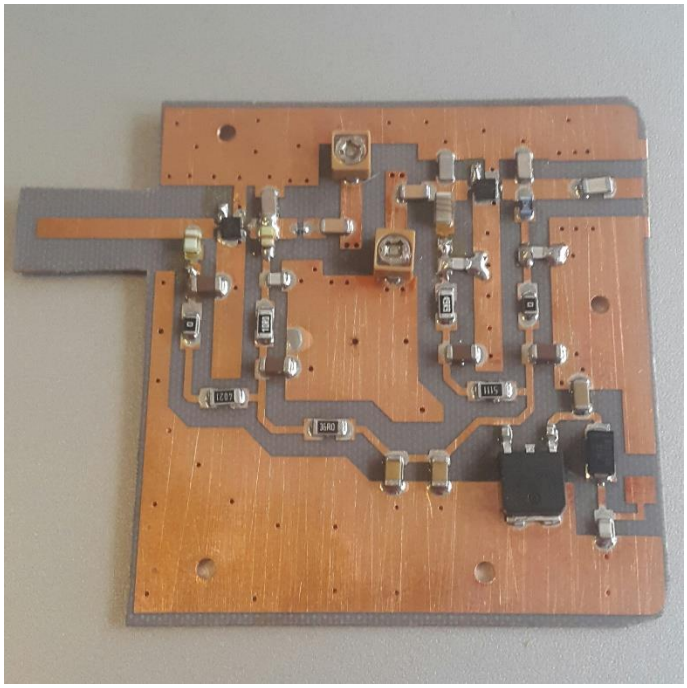

C.5 Complete LNA

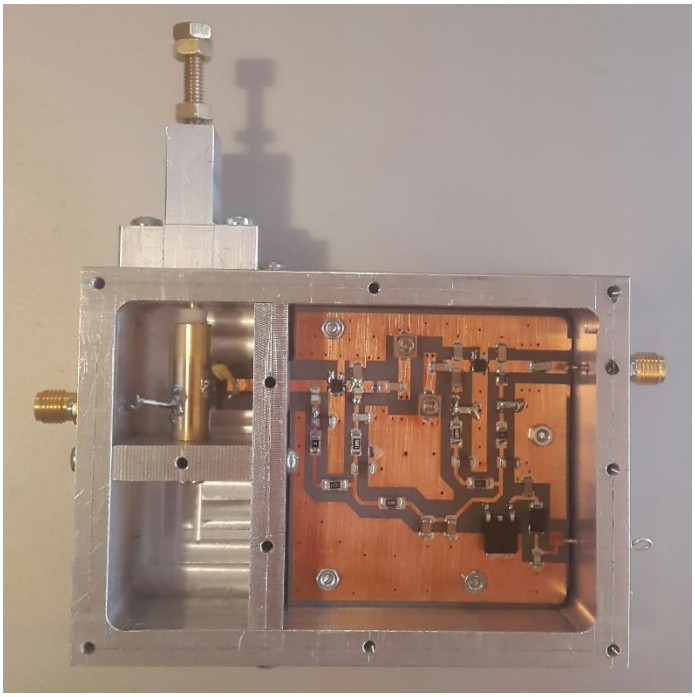

D LNA AND RESONATOR STRUCTURE

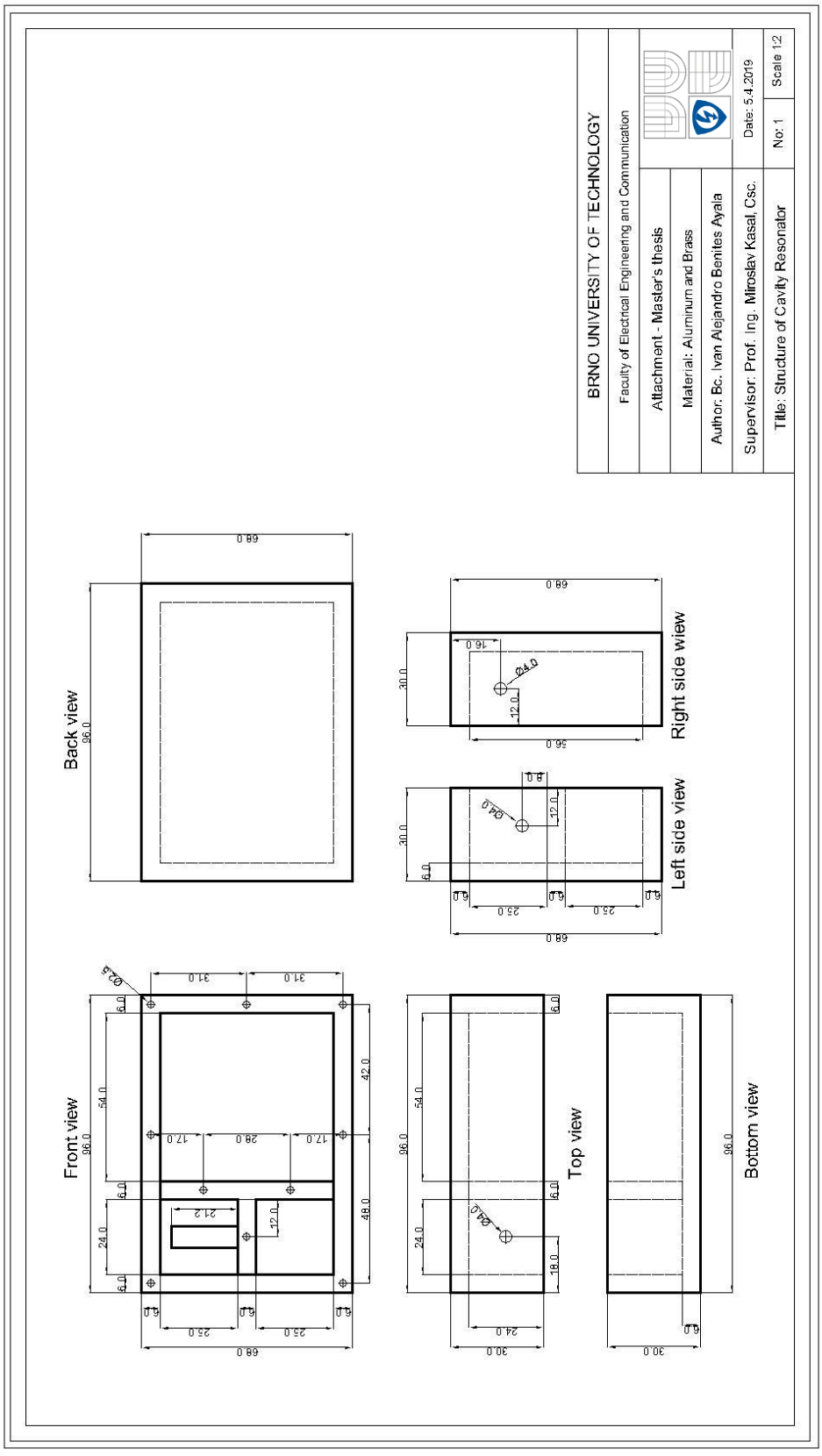

E LIST OF COMPONENTS

Label	Value	Case	Description
C1	2.7 pF	-	Ceramic capacitor
C2	4.7 uF	C1206k	Ceramic capacitor
C3	4.7 uF	C1206k	Ceramic capacitor
C4	33 pF	C0805	Ceramic capacitor
C5	1 pF	C1206K	Ceramic capacitor
C6	100 pF	C1206K	Ceramic capacitor
C7	1.4 pF - 3 pF	CTRIMTZBX4	Trimmer capacitor
C8	1.4 pF - 3 pF	CTRIMTZBX4	Trimmer capacitor
C9	100 pF	C1206K	Ceramic capacitor
C10	1.2 pF	C1206K	Ceramic capacitor
C11	100 pF	C1206K	Ceramic capacitor
C12	4.7 uF	C1206K	Ceramic capacitor
C13	4.7 uF	C1206K	Ceramic capacitor
C14	100 pF	C1206K	Ceramic capacitor
C15	1.8 pF	C1206K	Ceramic capacitor
C16	2.7 pF	C1206K	Ceramic capacitor
C17	4.7 pF	C0805K	Ceramic capacitor
C18	0.01 uF	C1206K	Ceramic capacitor
C19	1 uF	C1206K	Ceramic capacitor
C20	1 uF	C1206K	Ceramic capacitor
L1	33 nH	L0805	Inductor
L2	33 nH	L0805	Inductor
L3	2.7 nH	L0402	Inductor
L4	10 nH	L1206	Inductor
L5	8.2 nH	L0805	Inductor
R1	0 Ω	R1206	Resistor
R2	4.02 KΩ	R1206	Resistor
R3	10 Ω	R1206	Resistor
R4	49.9 Ω	R1206	Resistor
R5	5.11 KΩ	R1206	Resistor
R6	0 Ω	R1206	Resistor
R7	36 Ω	R1206	Resistor
D1	S1M-13-F	DO-214AC	Rectifier diode
IC1	PMA2-33LN+	2mm x2mm MC1631-1	Monolithic amplifier
IC2	PMA2-43LN+	2mm x2mm MC1631-1	Monolithic amplifier
IC3	LF50CDT	TO252	Voltage regulator
SMA	50 Ω	-	SMA connector
SMA	50 Ω	-	SMA connector